



Triglyceride accumulation and the cell cycle in chlorella  
by Robert Michael Thomas

A thesis submitted in partial fulfillment of the degree requirements for the degree of Master of Science  
in Microbiology  
Montana State University  
© Copyright by Robert Michael Thomas (1990)

Abstract:

Triglyceride (TG) storage lipid accumulates in microalgae during exposure to stresses which inhibit algal cell cycles. Such inhibition is typically induced by nutrient limitations such as depletion of nitrogen for green algae and silicate for diatoms. No direct mechanism has been described for low nutrient-induced lipid accumulation. It is proposed that TG accumulation in microalgae could be based on a synthesis/utilization pattern which is constitutive within the cell division cycle, as opposed to a specifically-induced synthesis of TG. Triglyceride accumulation occurs when a lag is induced in the cell cycle such that TG synthesis exceeds utilization. Historically, total lipids have been quantified and the cycling of TG independent of other lipid fractions has often been overlooked.

Recognizing the limitations of earlier researchers, trends in TG levels were examined using the neutral lipid (NL) specific fluorochrome, Nile Red, throughout complete cell cycles of synchronized cultures of *Chlorella* CHLOR1 under conditions of alkaline stress, nitrogen deprivation, and with monofluoroacetate (MFA) an inhibitor of the tricarboxylic acid (TCA) cycle. Alkaline pH stress, nitrate deprivation and TCA inhibition affects lipid accumulation by inhibiting the cell division cycle prior to TG utilization. Low levels of calcium were not found to have any noticeable effects on TG synthesis.

An accumulation of 2.5 to 5.5 times the initial NL level per cell resulted after 25 hours of culturing under alkaline conditions. Nitrogen deprivation yielded increases of 1.4 and 2.5 times the initial NL level after 36 hours and 14 days, respectively. In less than 30 hours, inhibition of the tricarboxylic acid (TCA) with MFA resulted in NL levels of 1.4 to 3.8 times the initial NL level per cell.

Radiolabeled acetate is assimilated at a constant rate into the neutral lipid fraction. Cultures with growth inhibited by MFA assimilated more radiolabel into neutral lipids and less radiolabel into the glyco- and polar lipid fractions than in control cultures.

TRIGLYCERIDE ACCUMULATION AND THE CELL CYCLE IN CHLORELLA

by

Robert Michael Thomas

A thesis submitted in partial fulfillment  
of the degree requirements for the degree

of

Master of Science

in

Microbiology

MONTANA STATE UNIVERSITY  
Bozeman, Montana

July 1990

N378  
T3665

**APPROVAL**

of a thesis submitted by

Robert Michael Thomas

This thesis has been read by each member of the thesis committee and has been found to be satisfactory regarding content, English usage, format, citations, bibliographic style, and consistency, and is ready for submission to the College of Graduate Studies.

7/19/90  
Date

*Kurt R. Coakley*  
Chairperson, Graduate Committee

Approved for the Major Department

7-3-90  
Date

*[Signature]*  
Head, Major Department

Approved for the College of Graduate Studies

9/26/90  
Date

*Henry J. Perovro*  
Graduate Dean

## STATEMENT OF PERMISSION TO USE

In presenting this thesis in partial fulfillment of the requirements for a master's degree at Montana State University, I agree that the Library shall make it available to borrowers under rules of the Library. Brief quotations from this thesis are allowable without special permission, provided that accurate acknowledgement of source is made.

Permission for extensive quotation from or reproduction of this thesis may be granted by my major professor, or in his absence, by the Director of Libraries when, in the opinion of either, the proposed use of the material is for scholarly purposes. Any copying or use of the material in this thesis for financial gain shall not be allowed without my written permission.

Signature

Robert M. Thomas

Date

September 4, 1990

**ACKNOWLEDGEMENTS**

I extend my special thanks to Dr. Keith Cooksey for his support , guidance, and encouragement on this project. I am grateful to all of the members of the Department of Microbiology for their willingness to share equipment and knowledge. I would particularly like to thank the other members of my graduate committee, Dr. Jim Cutler and Dr. Gordon McFeters for their advice and assistance with this project. I owe a special debt of gratitude to Dr. Jim Guckert for his inspiring enthusiasm and knowledge. I would also like to thank Barbara Cooksey for her methodological suggestions and friendship throughout this project. I would also like to express my thanks to the following people and groups:

All of the members of the MSU Biochemistry group, especially Dr. Larry Jackson for sharing equipment. The MSU Chemistry Department for use of plotting facilities. Dr. Pat Callis for use of the Spectrofluorometer and Dr. Scott Williams for sharing his expert knowledge of spectrofluorometry. Dr. Barry Pyle for discussions of viability studies and plotting assistance. Dr. Dave Ward for his interest and stimulating discussions about my project. Deb Berglund for flow cytometric analyses and suggestions. The Solar Energy Research Institute for funding this work and the Sigma Xi Grants in Aid of Research Foundation for funds to purchase a shaker.

## TABLE OF CONTENTS

	Page
ACKNOWLEDGEMENTS . . . . .	iv
LIST OF TABLES . . . . .	viii
LIST OF FIGURES . . . . .	ix
ABSTRACT . . . . .	xi
INTRODUCTION . . . . .	1
Project Goal . . . . .	3
Literature Review and Rationale . . . . .	4
Aquatic Species Program Overview . . . . .	5
Lipids as Storage Molecules . . . . .	10
Stress Effects and the Cell Cycle . . . . .	11
Biochemistry of Fatty Acid Synthesis . . . . .	15
Pyruvate dehydrogenase . . . . .	16
Regulation of Fatty Acid Synthesis . . . . .	18
Pyruvate Dehydrogenase . . . . .	18
Acetyl-CoA Carboxylase . . . . .	18
Fatty Acid Synthetase . . . . .	20
Desaturation of Fatty Acids . . . . .	21
Precursor Fatty Acids . . . . .	22
Two Pathway Model . . . . .	23
Utilization of Triglycerides . . . . .	25
Beta Oxidation or Membrane Lipids? . . . . .	25
The Lipid Trigger . . . . .	25
Sequential Synthesis of Lipid . . . . .	26
Some Hypotheses for Control of Lipid Synthesis . . . . .	28
Nitrate Deprivation . . . . .	28
Biosynthetic TCA Cycle . . . . .	28
TCA Inhibition . . . . .	30
Other Stress Conditions . . . . .	31
Calcium Effects . . . . .	31
Alkaline Stress . . . . .	31
Synchronous Cultures . . . . .	33
Induction of Synchrony in Various Systems . . . . .	36
Growth Parameters of Synchronous Cultures . . . . .	37
Viability . . . . .	39
Relative DNA Quantification . . . . .	40
MATERIALS AND METHODS . . . . .	42
Growth of Algal Cells . . . . .	42
Incubator . . . . .	45

TABLE OF CONTENTS--Continued

	Page
Analysis of Media Components . . . . .	47
Nitrate . . . . .	47
Calcium . . . . .	47
pH . . . . .	48
Culture Synchrony . . . . .	48
Viability . . . . .	49
Relative DNA Quantification . . . . .	50
Alkaline Stress . . . . .	52
Nitrogen and Calcium Deprivation . . . . .	52
Lipid Analysis Using Nile Red . . . . .	52
Microscopy and Photomicrography . . . . .	54
Radiolabeling Experiments . . . . .	54
Light/Dark Effects on Acetate Assimilation . . . . .	56
Influence of MFA on Lipid Accumulation . . . . .	56
Determination of Labeled Lipids . . . . .	58
<b>RESULTS . . . . .</b>	<b>62</b>
Synchrony . . . . .	62
Assessment of <u>Chlorella</u> Viability . . . . .	64
Plate Counts as a Viability Indicator . . . . .	64
Fluorescein Diacetate as a Viability Indicator . . . . .	64
Fluorometric Observation of DNA Levels with Hoechst Bisbenzimidazole Dye 33258 . . . . .	65
Cell Cycle Patterns of Triglyceride and DNA Levels Under Optimal Growth Conditions . . . . .	70
Visualization of Nile Red-Stained Triglyceride Droplets . . . . .	73
Alkaline Stress Effects on Neutral Lipid Accumulation . . . . .	76
Relative DNA Quantification by Flow Cytometry . . . . .	81
Nitrate and Calcium Deficiency . . . . .	86
TCA Inhibition with Monofluoroacetate . . . . .	89
TCA Inhibition with Monofluoroacetate Coupled to <sup>14</sup> C Acetate Uptake . . . . .	94
<sup>14</sup> C Acetate Assimilation into Lipid Fractions of Pre-labeled Cultures and the Associated Effects of TCA Inhibition by MFA . . . . .	98
<b>DISCUSSION . . . . .</b>	<b>102</b>
Synchrony . . . . .	103
Viability . . . . .	104
DNA Quantification . . . . .	105
Triglyceride Synthesis-Utilization . . . . .	108

TABLE OF CONTENTS--Continued

	Page <sup>a</sup>
Alkaline Stress . . . . .	109
Nutrient Limitation . . . . .	110
Nitrogen . . . . .	110
Calcium . . . . .	111
Monofluoroacetate . . . . .	111
Acetate Assimilation . . . . .	114
Practical Applications of Findings . . . . .	115
 CONCLUSIONS . . . . .	 118
 BIBLIOGRAPHY . . . . .	 120



## LIST OF TABLES

Table		Page
1.	Composition of Bold's Basal Medium . . . . .	42
2.	Assessment of Viability by Plate Count . . . . .	64
3.	Nitrate and Calcium Concentrations . . . . .	88
4.	Concentrations of Acetate Incorporated into Lipid Fractions . . . . .	95
5.	Cell Cycle Parameters and Observation Methods . . . . .	102
6.	Effects of Various Environmental Factors on TG Accumulation . . . . .	116

## LIST OF FIGURES

Figure	Page
1. Lipid Composition of Microalgae . . . . .	6
2. Proposed Neutral Lipid Accumulating and Non-Accumulating Conditions . . . . .	13
3. Pathways of Acyl Biosynthesis in the Chloroplast . . . . .	15
4. Control of Lipid Synthesis in Some Microalgae . . . . .	19
5. Scatterplots of Relative Cell Number for Asynchronous and Synchronous <u>Chlorella</u> .	63
6. Histograms of Fluorescein Diacetate Activity . . . . .	66
7. Bar Graph of Percent Viable Cells . . . . .	67
8. Relative Fluorescent Excitations of Unbound and Bound Hoechst 33258 . . . . .	68
9. Fluorescent Emissions of Unbound and Bound Hoechst 33258 . . . . .	69
10. Time Course of Staining <u>Chlorella</u> with Hoechst 33258 . . . . .	71
11. Cell Cycle of <u>Chlorella</u> at Neutral pH . . . . .	72
12. Fluorescent Micrographs of Nile Red-Stained <u>Chlorella</u> at 0.5 and 7.5 hours . . . . .	74
13. Fluorescent Micrographs of Nile Red-Stained <u>Chlorella</u> at 12 hours and 31 hours . . . . .	75
14. Alkaline Stress Effects on Cell Cycle and TG Levels . . . . .	77
15. Calibration Curve for Spectrophotometric Determination of Nitrate Concentrations .	79
16. Cell Cycle Parameters for Alkaline Stress and Control at Elevated Light . . . . .	80

LIST OF FIGURES--Continued

Figure	Page
17.	Flow Cytometer Fluorescence Behavior of Hoechst-DNA in pH 7 Cultures . . . . . 82
18.	Flow Cytometer Fluorescence Behavior of Hoechst-DNA in pH 10 Cultures . . . . . 83
19.	Flow Cytometer -- Percentages of Cells at the '2n' and '4n' Hoechst Fluorescence . . . . . 85
20.	Relative Nile Red and Cell Number for Low Nitrogen, Low Calcium, and Control . . . . . 87
21.	Relative Nile Red and Cell Number at 14 Days Low Nitrogen, Low Calcium and Control . . . . . 90
22.	Micrographs of Nile Red-stained Low Nitrogen, and Low Calcium Cultures at 14 Days . . . . . 91
23.	Micrograph of Nile Red-stained Control at 14 Days . . . . . 92
24.	Relative Nile Red, Hoechst Fluorescence and Cell Number for MFA-treated and Control . . . . . 93
25.	Assimilation of Radiolabeled Acetate into Lipid Fractions . . . . . 96
26.	Relative Nile Red and Cell Number for MFA-treated (40 mM) and Control Samples . . . . . 97
27.	Relative Nile Red and Cell Number for MFA-treated, Heterotrophic and Autotrophic Controls . . . . . 99
28.	Assimilation of Radiolabeled Acetate into Lipid Fractions (Label Added at Minus 40 Hours) . . . . . 101
29.	Acetate Saturation Curve . . . . . 131
30.	Monofluoroacetate Saturation Curve . . . . . 132

## ABSTRACT

Triglyceride (TG) storage lipid accumulates in microalgae during exposure to stresses which inhibit algal cell cycles. Such inhibition is typically induced by nutrient limitations such as depletion of nitrogen for green algae and silicate for diatoms. No direct mechanism has been described for low nutrient-induced lipid accumulation. It is proposed that TG accumulation in microalgae could be based on a synthesis/utilization pattern which is constitutive within the cell division cycle, as opposed to a specifically-induced synthesis of TG. Triglyceride accumulation occurs when a lag is induced in the cell cycle such that TG synthesis exceeds utilization. Historically, total lipids have been quantified and the cycling of TG independent of other lipid fractions has often been overlooked.

Recognizing the limitations of earlier researchers, trends in TG levels were examined using the neutral lipid (NL) specific fluorochrome, Nile Red, throughout complete cell cycles of synchronized cultures of Chlorella CHLOR1 under conditions of alkaline stress, nitrogen deprivation, and with monofluoroacetate (MFA) an inhibitor of the tricarboxylic acid (TCA) cycle. Alkaline pH stress, nitrate deprivation and TCA inhibition affects lipid accumulation by inhibiting the cell division cycle prior to TG utilization. Low levels of calcium were not found to have any noticeable effects on TG synthesis.

An accumulation of 2.5 to 5.5 times the initial NL level per cell resulted after 25 hours of culturing under alkaline conditions. Nitrogen deprivation yielded increases of 1.4 and 2.5 times the initial NL level after 36 hours and 14 days, respectively. In less than 30 hours, inhibition of the tricarboxylic acid (TCA) with MFA resulted in NL levels of 1.4 to 3.8 times the initial NL level per cell.

Radiolabeled acetate is assimilated at a constant rate into the neutral lipid fraction. Cultures with growth inhibited by MFA assimilated more radiolabel into neutral lipids and less radiolabel into the glyco- and polar lipid fractions than in control cultures.

## INTRODUCTION

Microorganisms growing under optimal conditions synthesize fatty acids primarily for esterification into membrane lipids -- phospholipids for plasma and organelle membranes; and in the case of photosynthetic organisms, glycolipids for chloroplast membranes. Under stressed conditions of nutrient limitation, lipid biosynthesis patterns change. Lipid accumulation has been reported for microalgae under a variety of nutrient limiting conditions including nitrogen (Suen, et al., 1987), silicate (Taguchi et al., 1987), selenium, (Doucette et al., 1987), and potassium (MacCarthy and Patterson, 1974). Triglyceride droplets have been observed in the cytoplasm of microeukaryotic algae under both optimal, nutrient-limited and alkaline stress conditions (Cooksey et al., 1987; Guckert & Cooksey, 1990; Thomas et al., 1990).

In microeukaryotic algae triglyceride (TG) droplets enriched in the precursor fatty acids 16:0 and 18:1w9c (Shaw, 1966) form in the cytoplasm (Cooksey et al., 1987; Guckert & Cooksey, 1990).

The ability of TG to accumulate in microalgae and its molecular similarity to mineral-oil derived hydrocarbons make these storage lipids an attractive renewable alternative fuel (Neenan et al., 1986).

Although lipid accumulation during nutrient limitation

is well documented, no direct biochemical mechanism for the change in metabolism resulting in TG accumulation has been determined.

Aside from these few observations of TG accumulation, most researchers have missed this TG cycling phenomena because they have typically quantified total lipids. As a result, the cycling of TG independently of the other lipid fractions was often overlooked (e.g. Shifrin & Chisholm, 1981). A likely reason such cycling was missed was that quantification of each lipid fraction at frequent points across the cell cycle is logistically very difficult. However, with the Nile Red (NR) technique developed earlier in our lab, observations of trends in TG levels are performed more easily (Cooksey et al., 1987).

Our investigations into cell cycle effects on triglyceride accumulation were inspired by earlier observations that alkaline pH stress resulted in TG accumulation in Chlorella independent of medium nitrogen or carbon levels (Guckert & Cooksey, 1990). Furthermore, we believe that some of the energy to fuel cell division may come from beta-oxidation and tricarboxylic acid (TCA) Cycle oxidation of the storage lipids. On this note, one would expect an inhibition of the TCA cycle to result in an elevated pool of acetyl-CoA available for fatty acid synthesis. Monofluoroacetate was chosen as an inhibitor of the TCA cycle (Cooksey, 1972).

### Project Goal

The goal of my thesis was to develop a better understanding of the effects of extracellular factors on the control of triglyceride accumulation. In order to do so, it is necessary to consider all aspects of lipid synthesis and turnover and the role of the cell cycle in TG dynamics. To accomplish this goal, the following objectives were established:

1. Confirm the existence of a constitutive triglyceride synthesis-utilization pattern across the cell cycle of synchronized cultures of Chlorella grown under optimal conditions of nutrient sufficiency and neutral pH.

2. Contrast the cell cycle dynamics of triglyceride levels in optimally grown cultures with TG levels in cultures subjected to artificially-induced extracellular stresses. The extracellular stresses employed include:

- a. alkaline stress
- b. calcium deprivation
- c. nitrate deprivation

3. Determine the effect of inhibition of the tricarboxylic acid cycle on triglyceride levels using monofluoroacetate (MFA), a recognized inhibitor of the TCA cycle.

The aim is to find a reproducible method to initiate TG accumulation.

In consideration of the logistics of operating a system for large-scale triglyceride production, it would be preferable to not wait for a medium component to disappear during normal cell growth (e.g. N-, Si-, Se-, etc.) or to have to remove cells from a replete medium and resuspend in a deficient one. The best "switch" would be one that works when it is added to the medium. This would not only be biochemically more convenient and decrease the likelihood of disturbances and artifacts, but it would also be more realistic in a large-scale production sense for efficient TG production. The work of Fisher and Schwartzbach (1978) indicate that an addition which decreases cell division rates, even temporarily, can have an influence on TG proportions. Such reliable control allows for analysis of the relationship between TG synthesis and TG accumulation in microalgae and the biochemistry involved therein.

#### Literature Review and Rationale

Microalgae are currently receiving considerable attention for their high concentrations of lipids of potential commercial value. Among the phytoplankton recognized as sources of useful lipids are Spirulina spp. and Chlorella spp. with their high contents of linoleic acid 18:3 and 20:5 respectively considered as a source of polyunsaturated fatty acids for use in health foods and



pharmaceuticals (Seto, 1984). Microalgae are also of interest for their Omega-3-fatty acids (w3) (Seto, 1984) and for their nonpolar lipids which may serve as an alternative source of hydrocarbon fuels (Neenan et al., 1986).

The term "lipid" is an operational term for molecules soluble in nonpolar solvents. The microalgal lipids include the triglycerides (TG) of cytoplasmic storage droplets, the glycolipid (GC) of chloroplast membranes and the polar membrane lipids (PL) (Figure 1). The term neutral lipid (NL) defines all those molecules of neutral polarity which are co-extracted in nonpolar solvents. Neutral lipids consist primarily of TG but also include some isoprenoids and hydrocarbons (Figure 1).

Triglycerides, particularly those in the more saturated straight chain form can be used as alternatives to conventional hydrocarbon fuels (Neenan et al., 1986). For this reason, TG can easily enter the fuel and other petroleum-based industries with minimal modification.

#### Aquatic Species Program Overview

The Aquatic Species Program was initiated in 1979 by the U.S. Department of Energy (DOE) and the Solar Energy Research Institute (SERI) as part of the renewable biofuels effort.

## LIPID COMPOSITION of MICROALGAE

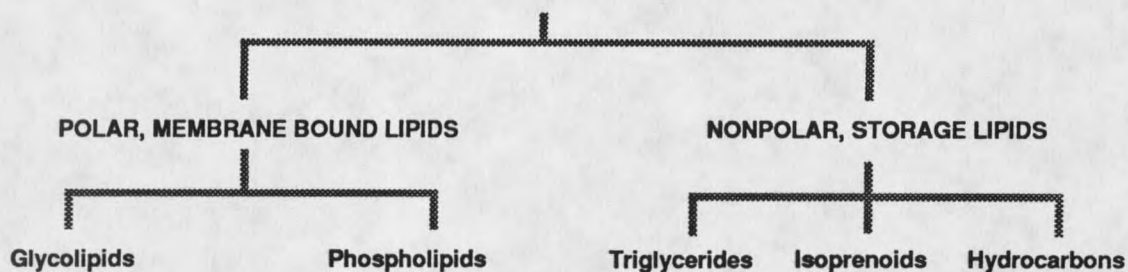


Figure 1. Lipid Composition of Microalgae.

Currently, 42% of the energy market in the U.S. is for liquid fuels and 38% of these fuels are imported (Bollmeier, 1989). It is estimated that up to 7% of the total current energy demand could be satisfied by the technology being developed in the Aquatic Species Program.

The DOE/SERI program emphasizes an initial commercial development of microalgal systems in the United States desert Southwest where there is an abundance of flat land and saline aquifers with few competing uses and high incident solar radiation. As the technology is envisioned today, microalgae would be grown in large, shallow ponds of saline water, harvested, and processed for the production of liquid or gaseous fuels including ethanol, triglyceride-based diesel fuel, ester fuel, methane, and gasoline (Neenan et al., 1986).

The goal of the SERI Aquatic Species Program is to attain a lipid accumulation of 50% of the algal cell dry weight, while maintaining high cellular productivity with yields of 50g dry weight per square meter of pond surface per day (Neenan et al., 1986). With this yield, 150 to 400 barrels of oil acre<sup>-1</sup> yr<sup>-1</sup> could be produced from microalgae (Bollmeier, 1989).

Recently, the program has been recognized for its potentially important role in reducing the dangers of the "Greenhouse effect," which is primarily due to the release of carbon dioxide in the combustion of fossil fuels. The utilization of this carbon dioxide through the mass culturing of photosynthetic organisms could significantly reduce the contribution to the greenhouse effect, particularly when microalgal fuel plants are coupled to fossil fuel plants as scrubbers of carbon dioxide from flue gases (Chelf & Brown, 1989).

In order to improve the cost effectiveness of microalgal-based fuels, the productivity of all system components must be enhanced. Specific advances in the engineering design of the mass culture system in photosynthetic efficiency, nutrient supply, harvesting and processing are ongoing.

Microalgal strains have been screened to select species that are temperature and salinity tolerant with high lipid production (Brown, 1989). Genetic engineering

techniques are also being investigated to improve microalgal production and lipid content.

Before genetic engineering is selected to enhance NL yields, it is essential to identify the genes and their associated gene products. Currently, the biochemistry of microalgal lipids is for the most part only surmised from what is known of the higher plants, higher animal liver, and bacteria.

Presently, SERI is investigating the potential for genetic enhancement of triglyceride yield by focusing on characterization of the acetyl-CoA carboxylase. Efforts are currently underway in SERI labs to determine a partial amino acid sequence for the enzyme and to produce antibodies against the enzyme in order to be able to examine the properties of the acetyl-CoA carboxylase-encoding gene (Roessler, 1990). The focus of the Aquatic Species Program microalgal genetics project is to obtain algae with altered lipid metabolism by mutagenesis and selection of mutants with desired traits. A second planned approach will utilize recombinant DNA technology to obtain algae with desired lipid accumulating properties with introduction of genetic material into the cell through protoplast production, particle bombardment, electroporation and other methods. Several of these approaches must first be customized for introduction of genetic material into microalgae. Selectable markers

which can be used to assess the efficiency of transformation must still be identified. Likewise, a system for introducing the genetic material for replication in microalgae must be identified. This can be achieved by integration of the plasmid into the host genome or with an autonomously replicating plasmid (Brown, et al., 1989).

Recognizing that microalgal recombinant technology is still in the early stages of evolution, the most promising short term techniques for maximizing TG accumulation are emerging in the recognition and understanding of the constitutive and induced cell cycle effects on TG accumulation. An empirical attempt at defining the conditions for maximizing TG accumulation would at best yield an inefficient system (Cooksey & Jackson, 1985). In order for the program to succeed, both the physiology and possibly the genetics of the organisms must be altered so that the cells become enriched in the desired fuel fraction. Additionally, aside from the product-oriented focus of the SERI program, this work has important implications in basic plant lipid biochemistry.

Microalgae are convenient models for higher plant biochemistry. The chlorophyte group of algae (Chlorella, Dunaliella) are considered to be evolutionary precursors of higher plants (Christensen, 1964; Peerasso et al., 1989) and are currently being utilized as models for

higher plant lipid biochemistry research (e.g. Lynch & Thompson, 1982).

### Lipids as Storage Molecules

In eukaryotic microorganisms and in animal cells, lipids may serve as energy storage molecules. Although the oxidation of extracellularly supplied fatty acids has been demonstrated in bacteria, there is little evidence that this process can be used for the breakdown of cellular lipids (Lennarz, 1966).

In animals the triglycerides are stored in specialized tissue, the adipose tissue; in oil-bearing plants they are stored in the seeds; in algae TG molecules are stored in droplets dispersed throughout the cytoplasm (Cooksey et al., 1987). Although some turnover of phospholipids has been demonstrated (Lennarz, 1966), the neutral lipids, particularly the glycerides, are the primary lipid storage molecules in eukaryotes.

Apparently, there is no evidence of such lipid storage capacity in bacteria (Lennarz, 1966). For lipids to serve as storage molecules in bacteria, a mechanism for the hydrolysis or oxidation of fatty acids is necessary.

Triglyceride is an efficient molecule for energy storage. During the controlled oxidation of fatty acids, ATP is generated yielding an energy supply equivalent of 38 kJoules of fatty acid catabolized, compared with 17

kJoules of carbohydrate or protein. Carbohydrate has to be stored in a bulky hydrated form, whereas three fatty acids can be stored per TG molecule in anhydrous form in animal adipose tissue or plant and microalgal TG droplets. The importance of TG is that they enable the animal, plant, or alga to store a much larger reservoir of energy than would be possible by storing carbohydrate or protein.

#### Stress Effects and the Cell Cycle

The accumulation of neutral lipids under stressed conditions of nutrient limitation (Suen et al., 1987; Taguchi et al., 1987; Doucette et al., 1987; MacCarthy & Patterson, 1974) and alkaline stress (Guckert & Cooksey, 1990) is well documented. Otsuka and Morimura (1966) and Fisher and Schwartzbach (1978) have suggested associations of TG levels with the cell cycle. It appears that NL accumulation is a result of the cell cycle being inhibited such that NL synthesis continues (during photosynthesis), but NL utilization decreases.

The term accumulation describes an important concept in this project. In fact, the word "accumulation" should be emphasized rather than synthesis in discussing changes in TG patterns across the cell cycle. Triglyceride accumulation is defined as:

$$\text{Accumulation} = \text{Synthesis} - \text{Utilization}$$

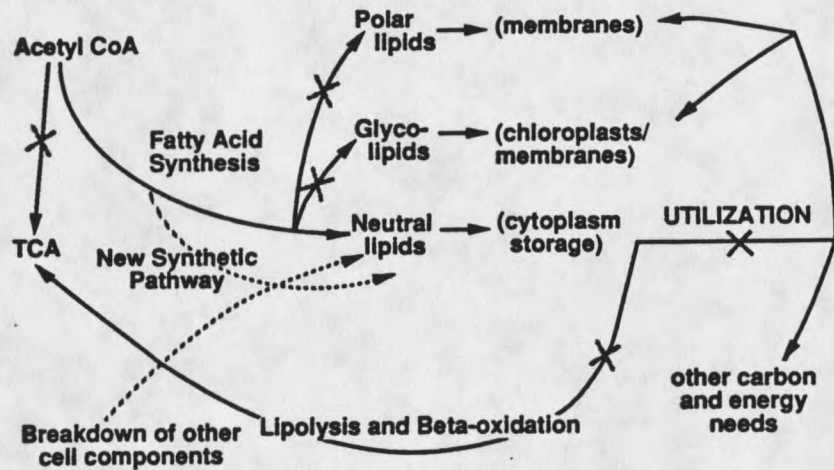
An accumulation of triglycerides occurs when TG synthesis exceeds the utilization phase of the cell cycle. This is an important distinction in comparison to earlier researchers who sought to identify a trigger for a separate TG synthesis pathway. Recognition of synthesis-utilization patterns is important when trying to define parameters for maximum TG production on an industrial scale.

Earlier work has suggested the existence of sequential synthesis patterns for different lipid classes during cell cycles (Sicko-Goad et al., 1988, Suen et al., 1988). An accumulation of TG may then be a result of an uncoupling of a synthesis/utilization pattern within one cell cycle (Figure 2). Studies with the diatom Thalassiosira have suggested that storage TG is utilized during cellular energy demand, such as during the dark or during cell division and an accumulation occurs when the cell has excess energy available as with non-dividing cells in constant light (Fisher and Schwarzenbach, 1978). A different study with Chlorella in 1966 (Otsuka & Morimura) reported a synthesis of TG throughout the photosynthetic growth phase of the cell cycle and a utilization during cell division. The concept of TG synthesis and utilization stages in the cell cycle appeared to be a very good hypothesis for the lipid accumulation story; but there was weak evidence to support this idea.



### NEUTRAL LIPID ACCUMULATING CELLS (Cell Cycle Inhibited)

*Neutral Lipid Accumulation = NL Synthesis - NL Utilization > 0*



### NEUTRAL LIPID NON-ACCUMULATING CELLS

*Neutral Lipid Accumulation = NL Synthesis - NL Utilization = 0*

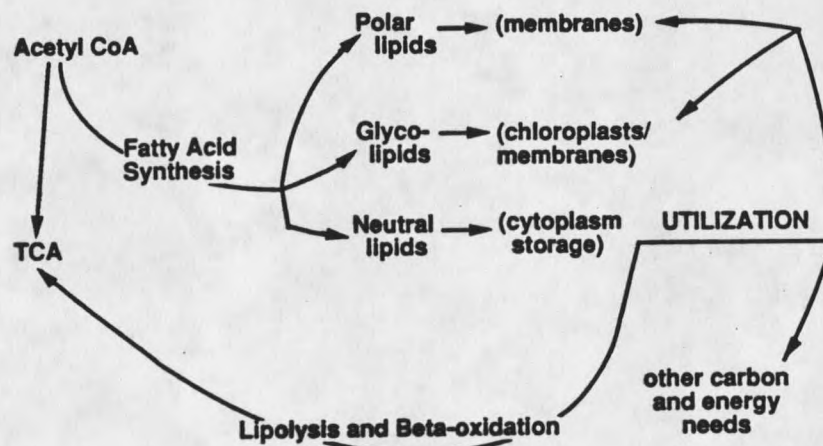


Figure 2. Proposed Neutral Lipid Accumulating and Non-Accumulating Conditions.

Tamiya (1963) published a map of the cell cycle-dependent stages of uptake of various nutrient elements in Chlorella. The data revealed that carbon or nitrogen depletion would result in inhibition during the early growth stages of the cell cycle before NL has accumulated.

Additionally, depletion of sulfur, which is assimilated during the ripening/post ripening stage (Tamiya, 1963) might increase cell yields of NL as cells would be inhibited during the cell cycle phase which results in the most NL accumulation just before cytokinesis.

The progression of the Chlorella cell cycle cannot be represented in the usual G1-S-M format since the S-stage of DNA synthesis is overlapped by the first mitotic event (M). The stages described by Otsuka and Morimura (1966) are compared with the more familiar G-S-M nomenclature. Using the Otsuka and Morimura nomenclature, neutral lipid is utilized in the post-ripening or L3-L4 phase.

Although lipid accumulation during nutrient limitation is well documented, no direct biochemical mechanism for the change in metabolism resulting in TG accumulation has been determined. A review of the known pathways for lipid biosynthesis will help to illustrate the hypothesized effects of nutrient deprivation and cell cycle inhibitors on lipid accumulation.

Biochemistry of Fatty Acid Synthesis (Figure 3)

The pathways of lipid synthesis in higher plants are essentially the same as in animals, yeasts, and bacteria (Gurr & James, 1975). Most research so far has indicated that the major site of fatty acid synthesis in plants is the chloroplast.

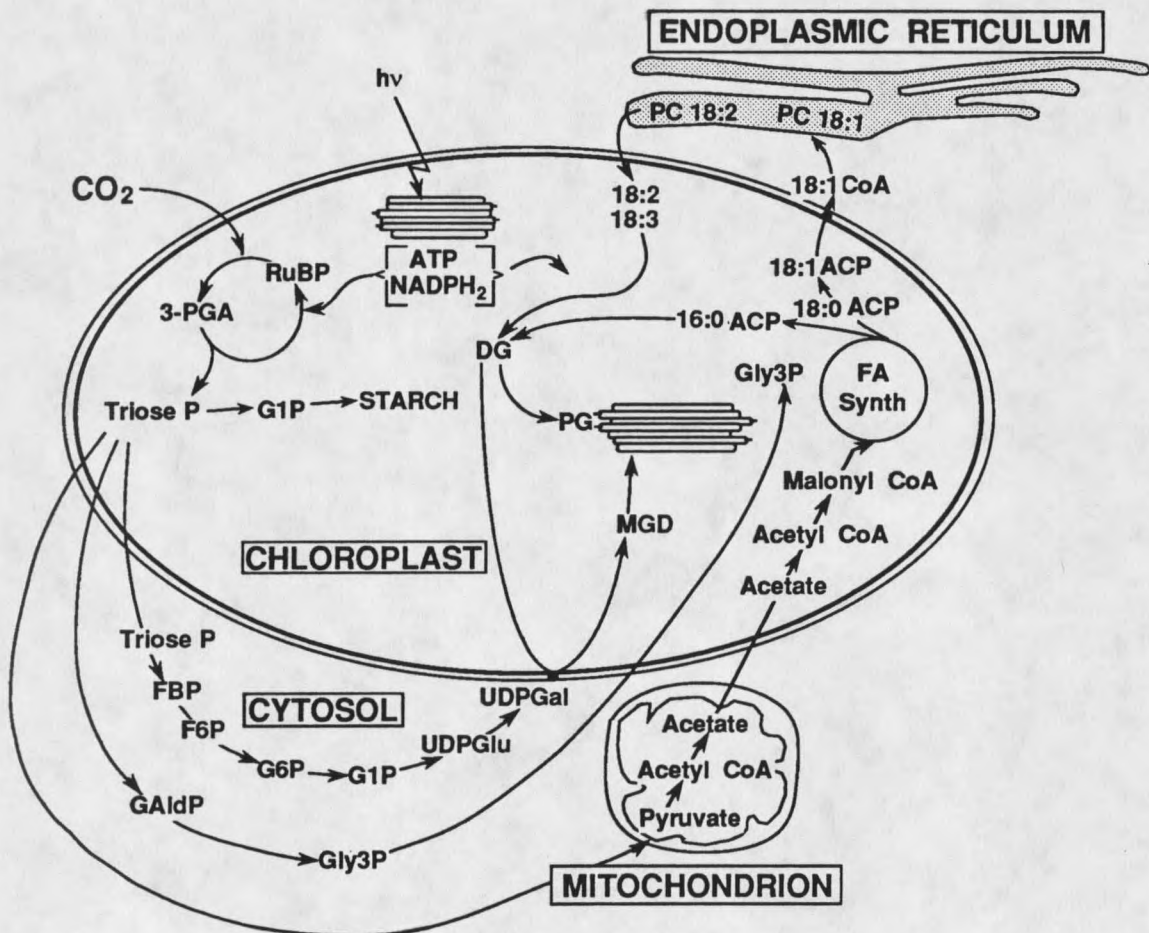
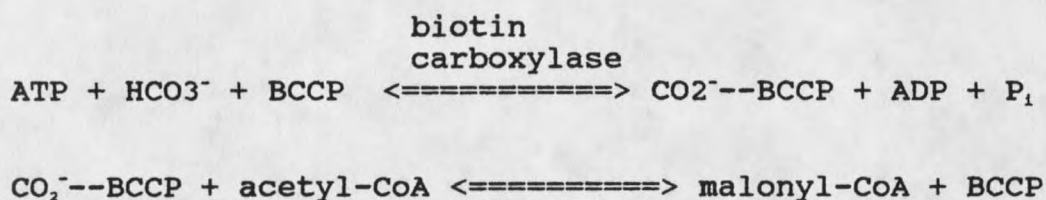


Figure 3. Pathways of Acyl Biosynthesis in the Chloroplast (from Murphy & Walker, 1982)

The first step in fatty acid synthesis is the carboxylation of the 2-carbon acetic acid to malonate. The acetate must be in an "activated" CoA thiol ester form. The carboxylation is catalyzed by acetyl-CoA carboxylase in which biotin is involved as a cofactor in carboxylation where it exists as a subunit of the acetyl-CoA carboxylase. In bacteria and higher plant chloroplasts, a biotin carboxyl carrier protein (BCCP) subunit exists for attachment to CO<sub>2</sub> by a separate subunit protein biotin carboxylase. As many as four subunits exist in the biotin carboxylase in algae (Roessler, 1990). One subunit of the acetyl-CoA carboxylase complex transfers the CO<sub>2</sub> from BCCP to acetyl-CoA to form malonyl-CoA (Gurr & James, 1975):



### Pyruvate Dehydrogenase

Most of the cell's acetyl-CoA is produced in the mitochondria from pyruvate during glycolysis (Liedvogel & Stumpf, 1982). The oxidation reaction is catalyzed by the pyruvate dehydrogenase complex (PDC). Little is actually known about the formation of acetyl-CoA in algae. However, information available on higher plant systems

indicates that the acetyl-CoA is hydrolysed in the mitochondria (Liedvogel & Stumpf, 1982) from where it may readily diffuse as free acetate into the chloroplast to be re-esterified to CoASH by an active acetyl CoA synthetase (Kuhn et al., 1981).

In spinach leaf chloroplasts, another acetyl CoA synthesizing system is found, i.e., acetyl CoA synthetase, suggesting that acetyl CoA may also be made from an intrachloroplastic partial glycolytic sequence (Murphy and Walker, 1982) (Figure 3). Work with spinach leaf chloroplasts (Liedvogel & Stumpf, 1982) and soybean cotyledons (Nelson and Rinne, 1977; Weaire and Kekinck, 1975) has revealed that since the mitochondrial membrane is impermeable to acetyl CoA, any acetate which reaches the chloroplast must be transported across the membrane as acetate, or other TCA intermediates.

In animals lipid synthesis occurs in the cytoplasm. Acetyl CoA is condensed with oxaloacetate to form citrate which is diffusible and reconverted to acetyl CoA in the cytoplasm (Gurr & James, 1975). In bacteria and seed proplastids, acetyl CoA is formed directly from pyruvate, with no intermediate transport compounds such as citrate involved in presenting the material to the carboxylase.

## Regulation of Fatty Acid Synthesis (Figure 4)

### Pyruvate Dehydrogenase

The activity of pyruvate dehydrogenase is regulated by NADH/NAD ratio, acetyl CoA/CoA ratio, TPP concentration, and by a phosphorylation/dephosphorylation sequence.

High levels of ATP would convert pyruvate dehydrogenase to the inactive form (Figure 4). In plants, the enzyme is inhibited by NADH, acetyl CoA and ATP, although the latter two effectors are possibly not active at physiological concentrations (i.e. in situ). Pyruvate dehydrogenase complex has been detected in pea chloroplasts and several types of protoplasts, but in a spinach there is conflicting evidence (Kuhn et al., 1981; Liedvogel & Stumpf, 1982).

### Acetyl-CoA Carboxylase

Citrate, isocitrate and fructose 1,6 bisphosphate activate acetyl CoA carboxylase in some animal systems (Rasmussen, R.K., and Klein, 1967; Hitchcock and Nichols, 1971). No activation occurs in yeast, E. coli or higher plants (Hitchcock and Nichols, 1971) (Figure 4). Hatch and Stumpf (1961) found the activators of the animal enzyme to be without effect on wheat germ AcCoA carboxylase. The situation in algae is again unknown.

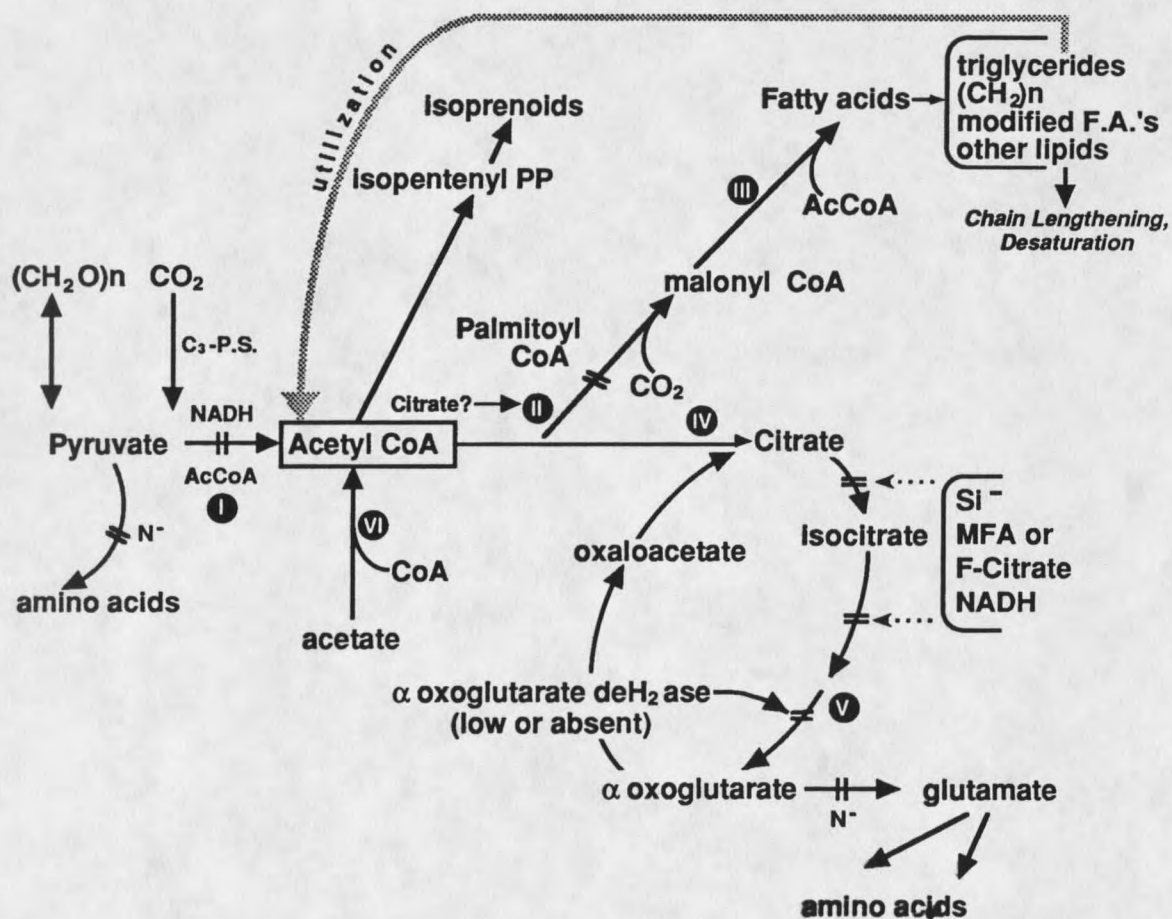


Figure 4. Control of Lipid Synthesis in Some Microalgae  
Legend:

(I)	Pyruvate Dehydrogenase		Inhibition
(II)	Acetyl-CoA Carboxylase	F-Cit	Fluorocitrate
(III)	Fatty Acid Synthase	PS	Photosynthesis
(IV)	Citrate Synthase	-->	Stimulation
(V)	Alpha Oxoglutarate dehydrogenase		
(VI)	Acetyl CoA Synthase		
(CH <sub>2</sub> ) <sub>2</sub>	Hydrocarbon		
(CH <sub>2</sub> O) <sub>2</sub>	Carbohydrate		
N <sup>-</sup>	Nitrogen Limitation		
Si <sup>-</sup>	Silicon Limitation		
MFA	Monofluoroacetate		

Malonyl CoA, the product of acetyl CoA carboxylase, inhibits the enzyme from avian liver. In vivo, however, this substance should be removed continuously by the fatty acid synthetase complex. Palmitoyl CoA, the ultimate product of the system, also inhibits the carboxylase (Figure 4).

### Fatty Acid Synthetase

In animal tissues, the activity of the fatty acid synthetase enzyme system and that of the acetyl CoA carboxylase, which catalyzes synthesis of malonyl-CoA, the substrate for the synthetase, are similar. Since the carboxylase is a highly regulated enzyme, there appears to be little point in regulating the synthetase activity directly. Fructose 1-6 bisphosphate is thought to activate the enzyme, however, the physiological significance of this is unknown (Figure 4).

The synthetase enzyme system is somewhat different in bacteria (E. coli) yeast, mammals and higher plants. Plants show a system intermediate between bacteria and yeast. The product of most plant systems is the acyl carrier protein-bound acyl derivative, however, not the free acid or its CoA derivative (Figure 3).

The fatty acid grows with the repeated addition of two carbon subunits to the carboxyl end. Only the two carbon atoms at the methyl end are derived from acetate (the



'primer' for the reaction) while the subsequent two carbon additions come from malonate (Liedvogel & Stumpf, 1982). When the primer is an acid with an odd number of carbon atoms such as propionate, then the resultant fatty acid chain is also of an odd-numbered chain length. When a branched chain primer is used, then a branched chain fatty acid results (Gurr & James, 1975).

In plants and algae, fatty acid synthesis is stimulated in the light because photosynthesis generates the ATP required for acyl activation and the NADPH needed in the reduction steps. Acetyl-CoA carboxylase has been demonstrated in plant tissues but an alternative route to malonyl-CoA is also available by the activation of malonate derived from oxaloacetate (Gurr & James, 1975):

CO<sub>2</sub>

Oxaloacetate ----> malonate ----> malonyl-CoA

#### Desaturation of Fatty Acids

The mechanisms by which plants and algae synthesize monounsaturated fatty acids is similar to that of animals in that it is an aerobic process involving an oxidase, molecular oxygen and NADH (or NADPH) to produce a double bond with the release of H<sub>2</sub>O (Erwin, 1973). Whereas animals can directly desaturate palmitic to palmitoleic and stearic to oleic acids, plants and algae are specific for stearyl-ACP and will not utilize stearyl-CoA or free

stearate; only 18:1w9 isomer is produced. Palmitoyl-ACP and other short chain fatty acyl-ACP compounds are chain-elongated but not directly desaturated. The 16:0 and 18:1w9c fatty acids are considered 'precursor' fatty acids since all other fatty acids are derived from desaturation and/or elongation of these molecules (Erwin, 1973).

### Precursor Fatty Acids

Shaw (1966) proposed that unicellular algae cultured under stress conditions such as nutrient deprivation accumulated lipids rich in oleic (18:1w9) and palmitic (16:0) acids. In comparisons with algae from optimal growth conditions, Shaw observed a higher relative proportion of polyunsaturated FA's in the optimal cultures with higher relative levels of the less saturated FA's in the stressed cultures. On this basis, he suggested that the polyunsaturated FA's served a structural role while the less saturated FA's served in a storage capacity. In support of this theory, the triglycerides have since been repeatedly shown to have a fatty acid profile dominated by 16:0 and 18:1w9 (Klyachko-Gurvich et al., 1969; Otsuka & Morimura, 1966; Guckert & Cooksey, 1990) while the glycolipids of the chloroplast membranes and the polar lipids of the plasma membranes are more polyunsaturated (Klyachko-Gurvich et al., 1981; Guckert et al., 1988; Guckert & Cooksey, 1990). Triglyceride droplets

accumulate in the cytoplasm of microalgae and are presumed to be the precursors to the prokaryotic and eukaryotic pathways. The concept of storing lipid molecules in a more saturated state of lower energy investment available to either of these pathways certainly makes teleonomic sense.

#### Two Pathway Model

A recent hypothesis for plant lipid biosynthesis helps explain the differential distribution of the precursor fatty acids on glycerolipids. The two pathway model (Frentzen, 1986; Roughan, 1987) proposes that the major products of chloroplast fatty acid synthesis are 16:0 and 18:1w9 (Roughan, 1987) (Figure 3). The first pathway, known as the prokaryotic pathway, occurs within the chloroplast and the major products are phosphatidyl glycerol with polyunsaturated 18-carbon acids at C-1 and 16:1w13t at C-2, and glycolipids with both polyunsaturated 18-carbon acids and 16-carbon acids (Roughan, 1987). All of these lipids are utilized in the chloroplast membranes. Most unicellular green algae would be categorized as 16:3 plants (Roughan, 1987) since they contain polyunsaturated 16-carbon acids as well as 18-carbon acids in their glycolipids (Klyach-Gurvich et al., 1981; Cho & Thompson, 1986).

The eukaryotic pathway occurs after the precursor fatty acids have been exported to the cell's endoplasmic reticulum (Frentzen, 1986). A branch point between the synthesis of the storage lipid TG and the membrane lipids presumably occurs at the diacylglycerol (DAG) pool.

After precursor fatty acids are esterified and further modifications to the complex lipid forms DAG, the lipid can either form polar and glycolipids with more highly unsaturated fatty acyl chains through a phosphatidyl choline intermediate, or triglycerides by an acyl transferase-catalyzed fatty acid esterification to the C-3 of DAG (Frentzen, 1986; Roughan & Slack, 1982). The polar lipids are utilized in the plasma and other membranes, while the glycolipids are actually formed in the chloroplasts following transport of an intermediate there (Frentzen, 1986). The triglyceride storage lipid forms droplets in the cytoplasm (Cooksey, 1987).

The concept of the precursor fatty acids (16:0, 18:1w9) being storage lipids and the polyunsaturated fatty acids being structural lipids has a biochemical basis, therefore, since TG can be formed from DAG with its esterified precursor fatty acids prior to further desaturation, although polyunsaturated fatty acids in TG are found in oil seeds (Frentzen, 1986) and diatoms (Opote, 1974).

## Utilization of Triglycerides (Figure 4)

### Beta Oxidation of Fatty Acids or Membrane Lipids?

The initial event in the utilization of triglycerides as an energy source is the hydrolysis of ester linkages by lipases. The individual fatty acids are then activated with the formation of a thioester bond between the carboxyl group of the fatty acid and the sulfhydryl group of CoA. The activated fatty acid is then degraded by the sequential removal of two-carbon acetyl CoA units generating NADH and FADH<sub>2</sub> (Gurr & James, 1975).

According to the theory proposed for alternative utilization of TG (Cooksey & Jackson, 1985), one of the three fatty acids found on the glycerol backbone of the triglyceride molecule would be lipase-cleaved and directed either to beta oxidation or esterification to a newly forming DAG molecule. The remaining DAG molecule would then be affixed with the appropriate glyco- or phospho-group designating the new molecule to a position in developing membrane lipids.

### The Lipid Trigger

Earlier work on microalgal lipid accumulation has sought to identify physiological cues which might "trigger" triglyceride synthesis (Walsh, 1984).

The so-called 'lipid-trigger' is a set of physiological circumstances that cause an organism to commit a large proportion of its metabolic energy to the synthesis of lipids. Nitrogen deficiency (Suen et al., 1987) and/or silicate deficiency (Taguchi et al., 1987) in growth medium reportedly cause such unidirectional shifts in metabolism. It has been known for many years that 'old' cultures of chrysophytes contain lipid droplets. A similar situation exists in silicate-starved diatoms (Werner, 1977). Likewise, Henderson & Sargent (1989) have reported a shift of the neutral lipid fraction to wax ester neutral lipids as the culture progresses from exponential to stationary phase. The mechanism for translation of nutrient deficiency and the subsequent shift in the metabolic machinery to a different series of metabolic reactions is not known. Furthermore, it is unknown why some algal cells make lipid, whereas others synthesize carbohydrate -- a reaction more familiar to bacteriologists. Neither is it true that all algae respond to N-deficiency in the same way (Ben-Amotz et al., 1985).

#### Sequential Synthesis of Lipid

The importance of a discussion of microalgal cell cycle lies in earlier work which has shown that the different lipid classes are synthesized in sequential

stages of the cell cycle. This includes sterols (Otsuka, 1963), sulfolipids, and phospholipids (Beck & Levine, 1977), glycolipids (Klyachko-Gurvich et al., 1981; Beck and Levine, 1977) and total lipids (Sundberg & Nilshammar-Holmvall, 1975; Sicko-Goad et al., 1988). It has also been suggested that TG accumulation is the result of a synthesis/utilization cycle within one cell cycle. Otsuka and Morimura (1966) reported that Chlorella ellipsoidea synthesizes TG throughout the photosynthetic growth phase of its cell cycle and utilizes it during cell division. Studies which have not reported such cycles have generally quantified total lipid accumulation and may have missed the cycling of TG independent of the synthesis of membrane lipids and cell biomass increases during the cell cycle (e.g. Reitz & Hamilton, 1967; Shifrin & Chisholm, 1981).

With these points established, there is no need to propose the existence of a lipid trigger to explain the fact that in certain growth conditions algal cells make more lipid than other materials. If compounds are metabolized by two pathways, one of which is only available when metabolic circumstances block the first and thus open the second, then this constitutes a 'triggering effect.' If both pathways are always open, but due to metabolic circumstances, one pathway is less active or completely inactive with the second taking the carbon flow from the first, then this does not constitute a true

triggering effect. Such is probably the case in algae whose general pathways of carbon metabolism are blocked or shifted either by Si or N-deficiency, i.e., there is no lipid trigger, lipid synthesis is merely a sink for excess recently-fixed carbon.

### Some Hypotheses for the Control of Lipid Synthesis

#### Nitrate Deprivation

The precise mechanism for the accumulation of lipids under nutrient stress is unknown. Based on studies of the yeast Candida 107, Botham and Ratledge (1979) have suggested that nitrogen deprivation restricts the TCA cycle by limiting the synthesis of adenosine monophosphate (AMP), an important cofactor for the NAD<sup>+</sup> dependent isocitrate dehydrogenase. With low levels of AMP (thus high ATP), high acetyl-CoA, high NADPH from the conversion of malate to oxaloacetate, and activation of the acetyl CoA carboxylase by citrate, fatty acid synthesis is stimulated. A similar hypothesis of a biosynthetic TCA cycle has been proposed by Cooksey and Jackson (1985).

#### Biosynthetic TCA Cycle

The central feature of the hypothesis is that the controlling step for TG accumulation exists at the level of acetyl-CoA (Figure 4). A secondary premise is that the



TCA cycle, a prime user of acetyl-CoA is reduced in activity (or even inhibited) by certain nutrient limitations, thus allowing acetyl-CoA to build up.

It is believed that, in microalgae and other autotrophs, a TCA cycle that is primarily biosynthetic may exist, with regulation of lipid synthesis at the level of AcCoA supply (Weitzman and Dunmore, 1969; Cooksey, 1972; Cooksey and Jackson, 1985). Likewise, under stress conditions, the TCA cycle, may be suppressed in activity or entirely inhibited. In diatoms, Si-deprivation causes a reduced flow of acetyl CoA to alpha-oxoglutarate resulting in a reduced pool of this compound and of glutamic acid -- the main source of nitrogen (as -NH<sub>2</sub>) for amino acid synthesis in glutamate -- alpha oxo- acid transaminases (Werner, 1968). Alpha-Oxoglutarate, which shuttles nitrogen through transamination in many organisms may accumulate in the absence of nitrogen or silicate, in the case of diatoms. In many obligate autotrophs, including at least one diatom (Smith, 1967; Cooksey, 1972), the TCA cycle is a biosynthetic pathway as it is in the case of anaerobically-grown E. coli (Weitzman and Dunmore, 1969), rather than an oxidative pathway. In a biosynthetic pathway, alpha-Oxoglutarate can inhibit citrate synthase rather than TCA inhibition by ATP which is seen in organisms possessing a complete, oxidative TCA cycle. As a result, in the biosynthetic-TCA type

organisms, a decrease in acetyl-CoA citrate by N-limitation increases acetyl-CoA and thus the activity of AcCoA carboxylase which in turn increases the concentration of malonyl-CoA the main ingredient for fatty acid synthesis (Cooksey and Guckert, 1988). The direction of carbon flow to lipid or carbohydrate depends on whether the pyruvate dehydrogenase continues to synthesize acetyl-CoA in the presence of excess acetyl-CoA. This concept is supported by studies where an increase in uptake of  $^{14}\text{C}$ -acetate is observed when aconitase is inhibited by fluoroacetate (Cooksey, 1972).

#### TCA Inhibition

Monofluoroacetate (MFA) was chosen as an inhibitor of the TCA cycle. In biological systems, MFA enters the TCA cycle as an analog of acetyl-CoA, condenses with oxaloacetate (catalyzed by citrate synthase) to form monofluorocitrate. Monofluorocitrate cannot undergo the dehydration step (catalyst = aconitase) to aconitate and thus the TCA cycle is inhibited (Vagelos et al., 1963) (Figure 4). It is also believed that citrate may serve as an effector for the acetyl-CoA carboxylase in fatty acid synthesis (Vagelos, 1963). Likewise, fluorocitrate may serve in this respect (Vagelos et al., 1963; Cooksey, 1972, 1974) affecting the synthesis of fatty acids and also inhibiting the activity of the TCA cycle (Figure 4).

## Other Stress Conditions

### Calcium Effects

Calcium deficiency has been reported to influence the development and cell shape in the green alga Scenedesmus obtusiusculus.

A report on the ultrastructural changes during cell division in synchronized cells grown in calcium deficient medium suggests that calcium deficiency inhibits the release of autospores, rather than decreasing the number of autospores actually produced (Nilshammar-Holmvall, 1975). Electron microscopic studies of synchronized cultures of Scenedesmus cultured in calcium deficient medium revealed about a 67% decrease in the average division number (Kylin, 1967; Nilshammar-Holmvall, 1975). Similar observations have been reported with Chlorella (Soeder & Thiele, 1967).

### Alkaline Stress

Observations of TG dynamics were conducted because earlier studies into microalgal lipid biochemistry indicated that in unbuffered medium, Chlorella accumulates TG prior to nutrient limitation (Guckert and Cooksey, 1990). This type of high pH stress results from photosynthetic consumption and has been shown to inhibit

the Chlorella cell cycle at the autosporangial stage (Malis-Arad and McGowan, 1982a) and result in an autoflocculation of algal cells (Sukenik and Shelef, 1984).

Additionally, it was observed that during pH stress, the fatty acid profile of triglycerides in Chlorella remains unchanged regardless of the amount accumulated with very little modification of the precursor fatty acids occurring after their esterification to the glycerol backbone. However, the membrane lipids (GL, and PL) are not stable under high pH conditions. Under high pH, glyco- and polar lipids have a higher proportion of the precursor fatty acids, suggesting a conservation of reducing ability in the stressed cells.

The above models for nutrient deficient and alkaline induced TG accumulation only suggest that various stress conditions will result in an increased synthesis of fatty acids. To date there exists no proven biochemical model which explains how saturated fatty acids can be esterified to TG then directed to membrane lipids and desaturated. Nor is there a clear explanation for the accumulation of TG under the influence of various stressors. At this point, it appears that a cell cycle lag induced by nutrient or alkaline stress, or TCA inhibition interrupts the cycle during a phase of constitutive TG synthesis. In other words, an interruption of the progression of the

algal cell cycle via deprivation of a particular nutrient, or metabolic activity does not result in absolute inhibition of all cellular functions, the synthesis of various photosynthates, for instance.

### Synchronous Cultures

Ideally, if one is to observe the specific physiological behavior of an organism, all of the cells in a culture should be in an identical state of maturation and metabolic activity. For this reason, researchers throughout the years have devoted tremendous effort to achieving synchrony in virtually all organisms studied (reviewed in Lloyd et al., 1982). A synchronous culture is the most efficient model of the behavior of a single cell. A declaration of synchrony is a very profound statement. Generally, cultures synchronized to between 60 and 85% of "complete" synchrony are considered to be very well synchronized (Lloyd et al, 1982).

### Procedures for Induction of Synchrony in Various Systems

Temperature-induced synchrony has been a popular method of controlling cell division ever since its introduction by Scherbaum and Zeuthen in 1954 (reviewed in Lloyd et al., 1982). More recently, a number of different systems involving various hot and cold temperature shocks at alternating time intervals have been developed for

inducing synchrony in various protozoa and bacteria (Lloyd, et al., 1982). The mechanisms by which temperature changes induce synchrony have been extensively reviewed (Lloyd et al., 1982).

Temperature changes under constant illumination have also been used to synchronize some algae such as Euglena (Padilla and Bragg, 1968; Terry and Edmunds, 1970), Chlamydomonas and Dunaliella (Wegmann and Metzner, 1971). Anacystis nidulans, a cyanobacterium, has also been synchronized by this technique (Lorenzen and Venkataraman, 1972).

Chemical inhibitors which block the cell cycle at specific points may also be used to induce synchrony (Lloyd et al., 1982). When exposed to such inhibitors, cells arrest at one stage of the cell division cycle. Subsequent removal from the inhibitor gives synchronous release and cell cycle progression. Many of the methods commonly used for mammalian cell lines usually lead to disruption of synthesis of macromolecules. For instance, the use of DNA synthesis inhibitors can dissociate the growth cycle from karyokinesis (Lloyd et al., 1982). Other methods reportedly minimize metabolic interference through the use of suboptimal inhibitor concentrations applied in short bursts (Lloyd et al., 1982).

Depletion and resupplementation of essential nutrients has also been used to achieve synchrony in bacteria, lower

eukaryotes and in some higher animal and plant cell cultures (Lloyd et al., 1982). Synchrony experiments have been performed with a variety of bacterial genera where stationary phase cultures are reinoculated into fresh medium (Lloyd et al., 1982).

In the algae, nutrient deprivation schemes include, Astasia longa starved for sulfate (Morimoto and James, 1969), silicon-starved diatoms (Lewin et al., 1966; Lewin, 1967; Coombs et al., 1967) and vitamin B<sub>12</sub> deficient Euglena gracilis (Sheheta and Kempner, 1979).

Division synchrony may also be achieved in a chemostat by adding a limiting nutrient periodically, where the period of addition is equal to the generation time (Lloyd et al., 1982). A number of chelating agents such as EDTA have been shown to be effective in inhibiting cell division in some fungi (Lloyd et al., 1982).

In phototrophs, synchrony can often be induced via the method pioneered by Tamiya et al., (1953) where suitable light/dark regimes result in entrainment of cell division (Lloyd et al., 1982; Spudich and Sager, 1980). A variety of regimes have been proposed for synchronizing green algae, some with unproven success. Tamiya's synchronization studies began with a 12:12 light:dark cycle (1953). However, it was later determined that the "synchronized" culture was not quite homogeneous with respect to the mode of cellular and nuclear division of

individual cells. As an alternative, Tamiya (1963) has described a technique relying on fractional centrifugation for isolation of small daughter cells for the synchronous culture. For this system, Tamiya used an initial 35 hour light period followed by a 17 hour dark period to ripen the cells and stimulate cell division. Synchrony was then maintained with a 17:9 light-dark (L:D) regime.

Several other researchers have investigated a variety of light-dark (L:D) cycles. Lorenzen et al. achieved complete synchrony of Chlorella with regimes of 16:12, 16:8, 20:20, and 24:12. Tamiya found the best results with the 17:15 regime. In all cases, the synchrony of growth and cell division is accomplished by repeating the light and dark cycle several times where cell growth ideally occurs only during the light period and division takes place primarily in the the dark period. Synchrony ultimately develops because cell division can occur in either light or dark while cell maturation or ripening occurs only in light.

Continuous synchrony is obtained by continuous dilution with fresh medium (Pfau et al., 1971) or by dilution once per cell cycle (Lorenzen, 1964; Padilla and Cooke, 1964; Padilla and James, 1964). Dilution to constant initial turbidity has also been demonstrated (Schmidt, 1974). Alternations of white light with yellow light through three cycles accompanied by an enrichment of



the gas phase with carbon dioxide also synchronizes several of the green algae (Lloyd et al., 1982).

#### Growth Parameters of Synchronous Cultures

Cell number is probably the most significant parameter for monitoring the growth synchrony of a culture. In a synchronized culture a period of constant cell number is followed by a rapid burst in cell number during the dark period where each fully ripened cell divides to four daughter cells (Tamiya, 1963).

Likewise, the dry weight and packed cell volume (PCV) of a culture increase exponentially during most of the light period in cell ripening. Dry weight decreases during the dark period due to respiration of storage products whereas packed cell volume stays constant. Cell weight increases again slightly after separation of the daughter cells.

Comparative observations of cell morphology and nuclear size can also allow for confirmation of cell synchrony. Tamiya et al. (1953, 1963) performed a detailed investigation of changes in cell morphology and nuclear division during the dark-light-dark cycle.

Tamiya et al. have found that insofar as a synchronous culture is to be used as a model for a single cell, the population must exhibit similar patterns of nuclear and cellular division. Using the Feulgen staining technique

to monitor the mode of nuclear division, the Tamiya group found the best overall synchrony in cultures started with homogenous cells obtained from fractional centrifugation.

For this project, an extensive investigation of the various elaborate means for achieving culture synchrony was avoided for the sake of time economy. A few observations of various light/dark regimes were made in an attempt to enhance the degree of synchrony. The Chen and Lorenzen (1986) 14:10 light/dark procedure for synchronization was chosen because it is recognized as a recently acceptable published method for achieving a substantially improved degree of synchrony over that of exponentially growing cultures. In any event, whatever level of synchrony is achieved in the commercial situation will be accomplished via entrainment by the natural, diurnal light/dark cycle. The most effective model for the physiological behavior of the organism in the outdoor facility will be that which most closely duplicates the natural variation in growth parameters.

The course of the Chlorella cell cycle begins with small daughter cells which grow with illumination, undergo nuclear division, or karyokinesis; then cell division, to form new daughter cells which repeat the cycle.

### Viability

With the realization that complete division may not have taken place over the course of one cell cycle (ie. two daughter cells versus four), viability studies were designed to assess whether the synchronization procedure was responsible for the low cell division number. Attempts at viability measurements using classical plate count techniques are presented in this thesis as is a procedure for flow cytometric estimation of viability using fluorescein diacetate (FDA).

In an effort to define the number of true cell divisions in one cell cycle, cell viability was estimated by flow cytometry using fluorescein diacetate (FDA). Flow cytometry has provided phytoplankton ecologists and physiologists with a system for rapid population analysis (Yentsch et al., 1983). Other researchers have coupled the use of FDA with flow cytometric measurements to assess the affect of pollutant stresses on viability of lichen algal cells (Berglund & Eversman, 1987).

Fluorescein diacetate (FDA) is a non-fluorescent molecule that crosses intact membranes. Nonspecific esterases break the ester bonds, producing fluorescein which is retained in viable cells (Berglund et al., 1987; Berglund & Eversman, 1988; Shapiro, 1985). The intensity of fluorescence depends on esterase activity in the cells,

intracellular pH, and integrity of cell membranes (Berglund & Eversman, 1988). Assuming that all viable cells exhibit esterase activity, a measure of cell viability is acquired.

#### Relative DNA Quantification

DNA levels were quantified fluorometrically and by flow cytometry with the bisbenzimidazole dye, Hoechst 33258 (Cesarone et al., 1979; Paul & Myers, 1982; Coleman, 1978; Coleman, 1979). Knowledge about the timing of DNA synthesis has aided in the understanding of regulation of the cell cycle (Slater et al., 1977). A comparison of NR units with plots of relative cell number and DNA units/million cells serves in positioning the trends in TG levels within the cell cycle.

Historically, correlations of DNA concentrations with cell cycle parameters typically involved extraction and measurement by UV-absorption (e.g, Senger and Bishop, 1966) or colorimetric analyses such as the diphenylamine (Senger & Bishop, 1966) or orcinol methods (Chen & Lorenzen, 1986). The new generation fluorochromes such as Hoechst and 4'-6'-diamidino-2-phenylindole (DAPI) are now being used in a wide variety of applications including aquatic ecosystems (Murray et al., 1986), plant protoplast development (Galbraith et al., 1981) and cytogenetic

observations in chlorophytes (Coleman, 1978; Coleman, 1979).

The use of flow cytometry to monitor rates of DNA synthesis across the cell cycle has been previously demonstrated using intact Saccharomyces cerevisiae cells stained with mithramycin (Slater et al., 1977).

## MATERIALS AND METHODS

Growth of Algal Cells

Chlorella CHLOR1 (Solar Energy Research Institute culture collection, Golden, Colorado) was grown in axenic cultures on Bold's basal medium (Nichols & Bold 1965) with the composition identified in Table 1.

Table 1. Composition of Bold's Basal Medium.

Constituent	Concentration mg L <sup>-1</sup>
NaNO <sub>3</sub>	250
CaCl <sub>2</sub> ·H <sub>2</sub> O	25
MgSO <sub>4</sub> ·7H <sub>2</sub> O	75
K <sub>2</sub> HPO <sub>4</sub>	75
KH <sub>2</sub> PO <sub>4</sub>	175
NaCl	25
EDTA	50
KOH	31
FeSO <sub>4</sub>	4.98
H <sub>2</sub> SO <sub>4</sub>	(1 mL L <sup>-1</sup> )
H <sub>3</sub> BO <sub>3</sub>	11.42
ZnSO <sub>4</sub> ·H <sub>2</sub> O	8.82
MnCl <sub>2</sub> ·4H <sub>2</sub> O	1.44

Table 1 (continued) Composition of Bold's Basal Medium.

Constituent	Concentration mg L <sup>-1</sup>
MoO <sub>3</sub>	0.71
CuSO <sub>4</sub> ·5H <sub>2</sub> O	1.57
Co(NO <sub>3</sub> )·6H <sub>2</sub> O	0.49

The medium was modified with nonmetabolizable biological buffer at a concentration of 10 mM. The buffers used were HEPES (N-2-hydroxyethylpiperazine-N'-2-ethane-sulfonic acid, pKa 7.5) and CAPS (3-[cyclohexyl-amino]-1-propanesulfonic acid, pKa 10.4) (Sigma Chemical Company). All cultures were HEPES-buffered except for alkaline-stress analyses in which the test samples were CAPS-buffered. Media and buffers were prepared with reagent grade water (Corning MegaPure System). The 100 mL cultures were incubated at 27°C in 250 mL flasks (Pyrex No. 4442 Culture Flasks or Bellco Delong Flasks) shaken at 100 rpm (Labline 3520 Junior Orbital Shakers).

Stock cultures of Chlorella were maintained on agar slants (2% Difco agar in Bolds Basal medium) in 16 x 125 mm screw cap culture tubes (Kimax, Kimble) incubated at room light and temperature levels. Transfers from the slants to 5 or 10 mL Bold's medium were made regularly.

When these cultures reached a cell density of approximately  $2 \times 10^6$  cells  $\text{mL}^{-1}$  aliquots were transferred to 250 ml culture flasks containing 100 mL medium. Experiments were performed with cultures only 3 or 4 generations removed in this serial transfer from the stock slants.

All flasks used for specific experiments were inoculated from exponentially growing cultures. At the start of each experiment several flasks were centrifuged (2460 g, 10 minutes, Beckman J2-21 Centrifuge) and the pellets were pooled together in a sterile carboy and resuspended so that the initial concentration of cells was  $10^5$  to  $10^6$  cells/ml. The cell suspension was then decanted into tared, sterile flasks where the various treatments were applied. For experiments involving artificially-induced nutrient deficiencies, the cells were pooled as described above then washed three times by centrifugation and resuspended in their respective buffered complete or nutrient deficient media.

In all conditions, cell concentrations were determined using a hemocytometer with a minimum of 400 cells counted for each sample. For construction of growth curves, 2 mL to 5 mL samples were fixed in 1.85% formalin and counted. Samples which could not be immediately counted were fixed and stored at 4 °C for later counting. For those experiments in which large volumes were required at each



sample point (for DNA, and/or FDA and TG analysis), 5 or 6 replicate flasks were maintained. In these situations the flasks were sequentially rotated through each sample collection so that only four flasks were sampled at each point. For radiolabeling experiments, the entire volumes of three replicate flasks were collected for analysis of lipid fractions.

In order to confirm that the cultures remained axenic two samples of each culture were collected with an inoculating loop and streaked onto separate plates containing bacterial check medium (2.0% agar, 0.5% yeast extract, and 0.5% glucose). The cultures were observed periodically for growth of bacterial or fungal colonies throughout one week of incubation in the dark at 27°C. Any cultures revealing contamination prior to the onset of an experiment were discarded. One instance in which bacterial contaminants were discovered after completion of the experiment is cited in the "Results" section of this document.

#### Incubator

All experiments were performed with cultures incubated in a controlled environment growth chamber (Percival). The incubator initially contained eight 40 inch cool white fluorescent tubes (Sylvania) and twelve 20 inch cool white fluorescent tubes (Sylvania) each arranged in banks of

four tubes vertically on the side walls of the incubator and horizontally over each of the two shelves. Light levels were measured with a Quantum Radiometer/Photometer (Model LI-185B, Li-Cor, Inc.) at 5 to 9 flask positions distributed across the entire shaker surface. Values for light readings are averaged and expressed in units of  $\mu\text{E}/\text{m}^2 \text{ s}^{-1}$ . Light levels were initially near  $100 \mu\text{E}/\text{m}^2 \text{ s}^{-1}$ . When it was realized that this light flux may have been inadequate for proper cell growth, the front and back walls of the incubator were lined with aluminum foil to achieve an increase in light reflected to the culture flasks. In addition, two fixtures containing 20 inch cool white fluorescent lights were added to each of the two shelves in the incubator. These light banks were supported at the same level as the shaker deck. With these modifications, light fluxes ranging from 150 to 170  $\mu\text{E} \text{ m}^{-2} \text{ s}^{-1}$  were achieved. Some preculturing was conducted in a different growth chamber (Lab-Line Instruments, Inc. Cat. No. 844) or in airlift fermenters (a 2 liter glass BRL Airlift fermenter, Bethesda Research Laboratories or a Custom 5 liter polycarbonate fermenter, Cerex Corporation) The fermenters were sparged with filtered atmospheric air at a rate of 2 liters per minute. Light fluxes reaching a maximum of  $290 \mu\text{E} \text{ m}^{-2} \text{ s}^{-1}$  were recorded at the inner wall of the fermenter vessels. Light levels in the Lab Line incubator typically ranged from 45 to 85  $\mu\text{E} \text{ m}^{-2} \text{ s}^{-1}$ . In

some cases, parent cultures for subsequent experiments were cultured in the low light intensity Labline incubator then transferred to the high light intensity Percival incubator for experimentation.

### Analysis of Media Components

#### Nitrate

The concentration of nitrate (as nitrate nitrogen,  $\mu\text{g mL}^{-1}$ ) was estimated for two experiments by the cadmium reduction colorimetric method using a commercially available test kit in which all reagents are combined into a stable powder pillow (NitraVer5 Nitrate Reagent; Hach, Inc. Loveland, Colorado; Nitrate Concentration Range: 0-30mg/L). The contents of one pillow were combined with 10 mL of media supernatant and vortexed for 10 seconds. After allowing five minutes for color development, absorbance was measured at 500 nm using a Gilford 2600 Spectrophotometer. A calibration curve was constructed using a series of dilutions of a 250 mg/L  $\text{NaNO}_3$  stock.

#### Calcium

Estimates of total calcium concentration were performed by the Chemistry Station Analytical Laboratory, Agricultural Experiment Station, Montana State University using the Environmental Protection Agency Method 215.1

(Atomic Absorption, direct aspiration; detection limit 0.10 ppm). Complete, and calcium-free noninoculated media and media supernatant collected at the completion of the experiment were provided for the analyses. Approximately 50 mL of cell-free medium were analyzed for each sample.

#### pH

Buffer, medium, and culture pH values were measured prior to and after each experiment. Before each experiment, the pH meter (Radiometer PHM53) was calibrated with pH 7, pH 9, pH 10, and pH 11 certified buffer solutions (Fisher Scientific). pH values for samples were then corrected from the calibration curve.

#### Culture Synchrony

Synchronous cultures of Chlorella were established by a method similar to that of Chen and Lorenzen (1986). Cells were subjected to a 14h:10h light/dark cycle followed by a 24h dark period and then continuous illumination throughout the monitoring period. Cells were centrifuged (2460 g, 10 min, 25°C) at the end of the extended dark cycle, and resuspended in the medium with the appropriate buffer. The Blumenthal Synchrony Index (Blumenthal and Zahler 1962) was used to estimate the degree of synchrony of those cultures exhibiting a doubling in cell number by the end of the monitoring

period. The Synchrony Index is calculated with the following equation:

$$F = N_t(N_0)^{-1} - 2^{(a/b)}$$

Where 'F' is the synchrony index; 'N<sub>t</sub>' is the final cell number; 'N<sub>0</sub>' is the initial cell number; 'a' is the time required for division; and 'b' is the typical generation time for the organism.

### Viability

Viability studies were conducted in an attempt to assess whether unexpectedly low cell division numbers were attributable to low culture viability. Culture densities were quantified by hemocytometer. The cultures were then serially diluted and spread on plates containing two different types of media, the bacterial check medium and Bold's Basal medium described earlier (American Public Health Association 1985). Use of these two types of media allowed for comparison of both the heterotrophic and autotrophic viability of the cultures with direct counts. Cultures inoculated onto bacterial check media were incubated in the dark at 27 °C (National Appliance Company) while samples on autotrophic media were incubated in the lighted growth chambers. When the colonies were sufficiently visible the number of colony forming units were compared with direct counts.

For one experiment, a comparison of dead versus live cells was performed on a Becton-Dickinson FACS 440 flow cytometer. Fluorescein diacetate (FDA) was used to quantify the number of cells exhibiting esterase activity in a method similar to that described by Berglund et al (1987). FDA (F-7378, Sigma) was diluted in acetone (1mg/2.4 mL stock solution). Stock solution was added to the cell suspensions to a final concentration of 10  $\mu$ M. Staining time was 10 minutes at room temperature. Cells were analyzed without washes. A Becton-Dickinson FACS 440 flow cytometer was used. Stained cells were excited at 488 nm with a Spectra-Physics 164-02 Argon-ion laser at 100 mW. Fluorescein emission signals were collected at 530 nm (30 nm bandpass). Results were collected as number of events versus the logarithm of the fluorescence intensity. 10,000 fluorescent events were recorded for each sample. Killed controls were fixed in 1.85% formalin.

#### Relative DNA Quantification

At each sample point, cells were fixed in 1.85% formalin in Bold's medium and their nuclei were stained with Hoechst Dye 33258 DNA (Paul & Myers 1982; Cesarone et al 1979; Coleman 1978; Coleman 1979). The method was modified in that the samples were stained at 1 mM Hoechst 33258, incubated for three hours at 37 °C

then washed and resuspended three times in the culture medium. Dye concentration, incubation time, number of washes, and excitation and emission spectra were defined in time course and concentration experiments for the particular microalga and spectrofluorometric system used (Spex Fluorolog model F211 spectrofluorometer equipped with a 150 W Xenon lamp). Stained cell fluorescence was measured as a function of time using a 1 second integration interval per point. Real time data acquisition and manipulation were performed using a Datamate microprocessor interface. Fluorescent intensity readings of the Hoechst-DNA complex were obtained for each sample at excitation and emission wavelengths of 357 and 471 nm, respectively.

A similar attempt at relative quantification of DNA was performed by flow cytometry. Hoechst-stained cells were washed as described above. The laser used was a Spectra-Physics 164-05. The cells were excited at 351/364 nm at 500 mW and the emission recorded with a 600 nm LP filter. Data collection techniques were similar to those described earlier for the FDA analysis. The fluorescence responses of the Hoechst-DNA complex were presented as contour plots.

### Alkaline Stress

Two separate experiments were conducted to observe the effects of alkaline stress (CAPS buffer, pH 10) on cell cycle progression and TG levels. Control cultures were maintained at neutral pH (HEPES buffer, pH 7).

### Nitrogen and Calcium Deprivation

The effects of nitrate and calcium deficiency on TG accumulation and the cell cycle of Chlorella were observed in simultaneous experiments. Nitrate and calcium deficient media were prepared according to the method of Nichols and Bolds (1965) without the addition of sodium nitrate ( $\text{NaNO}_3$ ) or calcium chloride ( $\text{CaCl}_2$ ), respectively. Nitrate and calcium analyses were performed by the procedures described above. In order to assess any secondary effects of sodium or chloride deficiencies due to elimination of  $\text{NaNO}_3$  or  $\text{CaCl}_2$  from the media, one flask of each test series was restored to the appropriate sodium or chloride concentration with  $\text{NaCl}$ .

### Lipid Analysis Using Nile Red

The Nile Red estimation of triglyceride lipid was performed according to fluorometric methods developed by Cooksey et al (1987). To monitor triglyceride accumulation over time, 5 mL aliquots were transferred



from the algal culture to 13 x 100 mm glass cuvettes (Fisher cat. no. 14-385-900B) and assayed directly with Nile Red. The fluorescent response was quantified by fluorometry 8 minutes after the sequential addition of Nile Red (20 uL of 250 ug uL<sup>-1</sup> in acetone) and acetone (180 uL). Nile Red (9-diethylamino-5H-benzo[alpha]phenoxazine-5-one) was obtained from Molecular Probes (Junction City, Oregon) or Kodak (Rochester, New York). The standard used was 2.8 um Nile Red-stained monodisperse latex particles (a gift of Dr. C.J. Wang, Pandex Laboratories, Mundelein, Illinois). The working standard was made up to a concentration of  $5.88 \times 10^5$  beads mL<sup>-1</sup>. Five mL of this standard was used to calibrate the Turner Model 10 fluorometer at a setting of 5.0 (net scale expansion = 3.16). The filters were a  $480 \pm 10$  nm excitation filter and a  $580 \pm 9.8$  bandpass emission filter. The Nile Red data were expressed in arbitrary units defined such that the working standard represents 100 units mL<sup>-1</sup>.

When it was realized that adherent dye molecules may have interfered with fluorometric results a more thorough method for cleaning the cuvettes was begun. Before use, the cuvettes were washed in Micro soap, rinsed three times with tap water and boiled and rinsed twice with reagent grade water, then rinsed three times with bulk acetone (Chemistry Stores, Montana State University).

### Microscopy and Photomicrography

Photomicrographic records of the Nile Red response due to TG droplets for each treatment were taken for various sampling times throughout the monitoring period. The algal cells were viewed at 200x and 400x and recorded both with light and epi-fluorescent illumination using a 450 - 490 nm excitation filter, a 510 dichroic mirror and a 520 nm barrier filter. Photomicrographs were taken with a Nikon Optiphot microscope equipped with automatic exposure utilizing Ektachrome film (160 ASA, tungsten) set at ASA 80.

### Radiolabeling Experiments

In an effort to further substantiate the lipid dynamics observed fluorometrically, a series of experiments were designed to monitor incorporation of 2-<sup>14</sup>C acetate into the various lipid fractions.

Acetate concentration was defined with the construction of a saturation curve (Appendix) where the same amount of radiolabeled 2-<sup>14</sup>C acetate was added to a series of flasks (10 mL side arm reaction flasks) containing 2 mL aliquots of an exponentially growing algal culture and a range of unlabeled NaOAc concentrations. 2 uCi 2-<sup>14</sup>C NaOAc (50 mCi/mole) (ICN Radiochemicals) was added to each flask. Three replicate flasks were prepared

for each concentration of acetate (ranging from 0 to 50 mM). The flasks were then incubated for 3 hours. Assimilation of acetate into whole cells was measured in a method similar to that of Cooksey (1972). To remove nonassimilated radioactivity, the intact cells were washed on 2 uL glass fiber filters (Millipore) with 30 mL Bold's medium to remove unincorporated radiolabel. This wash volume was defined in a test where a series of 2 mL aliquots were taken from the same culture pre-labeled with  $^{14}\text{C}$  acetate, incubated for 3 hours then washed on glass fiber filters. The various treatments consisted of wash volumes of either 5, 10, 20, 30, 40, or 50 mL of medium. Three replicates were used for each treatment. Three blank filters were washed with 30 mL Bold's to determine nonspecific label retention. For all experiments where whole cells were washed on filters, the filters were air dried, placed in 5 mL Ecolume (biodegradable) scintillation cocktail (ICN Biochemical Company, cat. no. 882470) and counted in a Packard Tri-Carb Liquid Scintillation system. External standards (Amersham-Searle, model 180060 Liquid Scintillation Carbon-14 Quenched Standard Set) were used to estimate counting efficiency for determination of disintegrations per minute (dpm). The minimum sufficient wash volume was defined as the point where the scintillation counts per minute remained unchanged with increasing wash volumes.

### Light/Dark Effects on $^{14}\text{C}$ -Acetate Assimilation

The effects of the synchronization regime on acetate assimilation was also assessed. In order to determine whether the system would remain saturated with radiolabel when subjected to the synchronization protocol described above, 1.44  $\mu\text{Ci}$  2- $^{14}\text{C}$ -acetate (ICN Radiochemicals; specific activity 50  $\text{mCi}/\text{mMole}$ ) and 40  $\text{mM}$  NaOAc (an excess defined in the earlier saturation experiment) was added to 100 mL of an exponentially growing culture (diluting the specific activity to 0.36  $\mu\text{Ci}$  per  $\text{mMole}$  acetate assimilated). The culture was then transferred in 3 mL aliquots to thirty reaction flasks. Three flasks were sampled at 10 different monitoring times beginning at 40 hours prior to the onset of the continuous light period. The cells were then washed and the radioactivity was determined as described above.

### Influence of MFA on Lipid Accumulation

Three separate experiments were designed using MFA at concentrations of 40  $\text{mM}$  for two experiments and 25  $\text{mM}$  for a third experiment. The MFA was added to the cultures at the onset of the continuous light period. The concentrations of MFA were defined in a saturation experiment involving assimilation of 2- $^{14}\text{C}$ -acetate into whole cells at various concentrations of MFA in a method

described by Cooksey (1972). The MFA saturation experiments are similar in design to those described earlier for determination of acetate concentration. In determining the concentration of MFA, a saturating acetate concentration (40 mM) was chosen and MFA concentrations ranging from 0 to 40 mM were used (Appendix). The flasks were preincubated for 15 minutes before the addition of acetate and radiolabel. The combination of radiolabeled and unlabeled acetate in the medium yielded a specific activity of 25 uCi per mMole acetate assimilated.

For two experiments, control flasks were maintained under identical conditions without acetate and inhibitor. 40 mM MFA was added to the experimental series of flasks for these experiments at the onset of the continuous light period (time zero). For one of these experiments, additions of radiolabeled acetate (1.44 uCi/100 mL; 50 uCi/uMole initial specific activity), and 40 mM acetate (diluting the specific activity to 0.36 uCi/mMole acetate) were made at time zero in an effort to observe rates of lipid synthesis. A third experiment with MFA was designed to monitor lipid dynamics in a system beginning the continuous light period saturated with radiolabeled acetate. An additional series of control flasks containing 40 mM acetate was established for this final MFA experiment since it was realized that photoheterotrophic growth on acetate may affect

triglyceride dynamics in unstressed cultures. In each experiment involving monofluoroacetate, four replicate flasks from each treatment were analyzed at each sample point.

#### Determination of Labeled Lipids

Entire flask volumes of three replicate samples were collected for lipid analysis at critical points of inflection in TG levels which were identified in earlier fluorometric analyses with Nile Red. The samples were pelleted and transferred to 16 x 125 mm culture tubes tared (Allied-Fisher Model 7303DA balance and Mettler H54AR) to the nearest milligram. The samples were frozen overnight at -20 °C then lyophilized at  $\leq 100$  millitorr and -55 °C for 14 hours. The culture tubes containing the dried pellets were then reweighed. Tube weights were the means of three separate weighings. The gram dry weights of the samples were determined by the difference in tube weights.

Lipid extraction was performed by the Bligh and Dyer (1959) chloroform/methanol/water technique as modified with phosphate buffer by White et al (1979). All glassware was washed in Micro laboratory soap, rinsed with tap water, rinsed with distilled water, dried, methanol and chloroform rinsed (ACS certified, Fisher Scientific)

and soaked overnight in first phase Bligh and Dyer (B/D). First phase B/D consists of capillary gas chromatography (CAPGC) grade solvents (Burdick and Jackson) and reagent grade water which has been stored over chloroform. First phase B/D contains chloroform:methanol:50 mM phosphate buffer in the volume ratios of 1:2:0.8. The 50 mM phosphate buffer is made with 8.7 g  $K_2HPO_4$  per liter water, adjusted with 1 N HCl (J.T. Baker Chemical Company) to pH 7.4. Lipids were extracted and fractionated in the following five day procedure:

DAY 1: Algal pellets were transferred to 250 mL glass separatory funnels and extracted overnight in 133 mL first phase B/D.

DAY 2: Solvent phases were split with the addition of 35 mL chloroform and 35 mL water.

DAY 3: The lower chloroform (lipid-containing) phase of the separatory funnels was through Whatman 2V paper into a round bottom flask (24/40 mm, 300 mL, Pyrex Corporation). The solvent was removed using a quickly spinning roto-vap (Rotovapor R Model, Buchi) operated at 400 to 500 mm Hg vacuum (General Electric model 5KH33DN16X vacuum pump). The flask was quickly spun in a water bath maintained at 37 °C. When all the

solvent was evaporated, the system was open to atmospheric pressure under nitrogen. Four 2 mL washes of transfer solvent (hexane:chloroform, 4:1) were used to transfer the lipids to a test tube. The solvent was removed from the test tube under minimal nitrogen flow (N-Evap model 111, Organomation Associates, Inc.) in a 37 °C water bath (Model 220, National Appliance Company). The dried lipids were stored overnight in a -20°C freezer.

DAY 4: The lipids were fractionated by silicic acid column chromatography (SAC)(Guckert et al 1985). Columns were prepared from wide-bore Pasteur pipets which were glass wool plugged and rinsed with chloroform. The stationary phase used was activated (120 °C for at least 2 hours) 100 to 200 mesh Biosil A. 0.5 g stationary phase was added to the columns and cleaned with 10 mL washing grade chloroform. The room temperature lipid was transferred to the head of the column in a minimal volume of CAPGC grade chloroform. Once loaded, 10 mL chloroform was added and the neutral lipids were dripped from the column into screw cap test tubes. Next, 10 mL acetone was used to remove the glycolipid fraction into another tube. Finally, 10 mL methanol was used to remove the polar



lipids into a third tube. All lipid fractions were dried as described above and stored at  $-20\text{ }^{\circ}\text{C}$ .

DAY 5: Dried lipid fractions were resolvated in 100  $\mu\text{L}$  of a 1:1 methanol-toluene solution. 50  $\mu\text{L}$  of the sample were then put into 5 mL Ecolume scintillation cocktail and tested for radioactivity as described above.

**RESULTS**Synchrony

Cultures subjected to a 14h:10h light/dark regime followed by a 24 hour dark period and then continuous illumination exhibited a greater degree of synchrony than cultures incubated under constant 12h:12h light/dark cycles (Figures 5A & 5B). In the synchronized cultures a scatterplot of cell number versus cycle time reveals a flat growth curve until the point of cell division where the curve resembles a step function reaching a plateau at the completion of the cell cycle (Figure 5b). With this method of synchronization, control cultures of Chlorella began to divide after the fourteenth hour of reillumination achieving a doubling in cell number by the 22nd hour. Cultures appear to remain relatively well synchronized for at least one additional cell cycle (Figure 5B). In contrast, cultures not subjected to the extended dark cycle displayed a relatively flat growth curve shortly after inoculation but quickly became more dispersed in cell number (Figure 5A). Synchronized cultures experienced a  $1.54 \pm .078$  fold increase in cell number during the extended dark period.

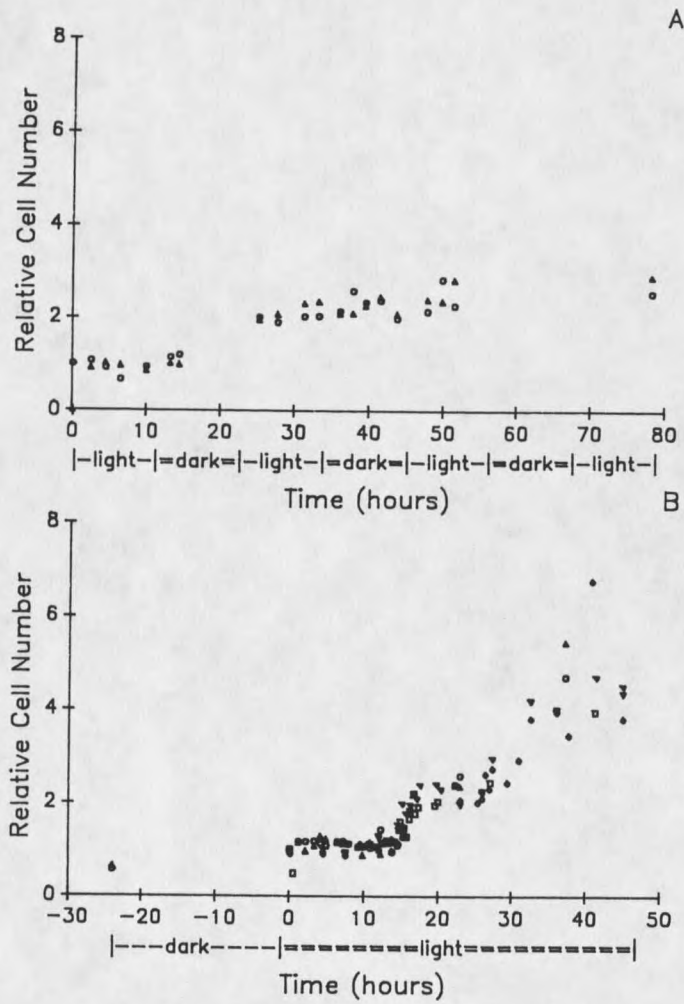


Figure 5. Scatterplots of Relative Cell Number for asynchronous *Chlorella* (A) and *Chlorella* synchronized by 14h:10h light:dark & extended dark regime. Numbers in (A) are from two independent studies, (B) nine independent studies.

Assessment of Chlorella Viability

Plate Counts as a Viability Indicator

Samples of Chlorella diluted and grown on solid medium using the spread plate technique (McFeters, 1985) yielded colony forming units correlating to less than 50 percent of the cell density observed by hemocytometer. The percentages of the direct counts which appeared as colony forming units on agar prepared with Bold's medium or Bacterial Check medium are presented in Table 2.

Table 2. Assessment of Viability by Plate Counts

Medium	Percent of Direct Count
Bold's	49.37 ± 15.1
Bacterial Check	42.53 ± 7.1

Note: Percentages are for 9 replicates in each medium. Exponentially growing cultures were used to prepare pread plates. Dilutions of  $10^{-3}$  and  $10^{-4}$  of exponential cultures were used to prepare spread plates. 12 to 15 days were required before colonies were large enough to count.

Fluorescein Diacetate as a Viability Indicator

For a separate series of samples, cell viability was estimated by flow cytometry using fluorescein diacetate

(FDA). Histograms of the number of fluorescein containing events versus fluorescence intensity are presented in Figure 6. The lower intensity autofluorescence is easily distinguished from fluorescein emissions (Figure 6). The percentages of the 10,000 fluorescent events exhibiting fluorescein activity are translated from the histograms as a bar graph (Figure 7). Only  $78 \pm 13$  percent of the cells just entering the light after an extended dark period displayed esterase activity. A peak in esterase activity of  $99 \pm 0.3$  percent occurred at the sixth hour. The cultures ended the cycle at  $88 \pm 3.7$  percent esterase activity (Figure 7).

Fluorometric Observation of DNA Levels  
with Hoechst Bisbenzimidazole Dye 33258

Unbound Hoechst stain has excitation and emission wavelengths of 336 nm and 490 nm, respectively (Figure 8). The Hoechst-DNA complex has excitation and emission spectra of 357 and 471 nm, respectively (Figure 9). Fluorescent emissions by unbound Hoechst stain interfere with emissions from bound Hoechst (Figure 9).

Since DNA levels were quantified at the maximum fluorescent intensities it was important to remove any additive fluorescence interference by unbound stain. A time-course of staining indicates that cells must be incubated for almost 3 hours before fluorescence levels

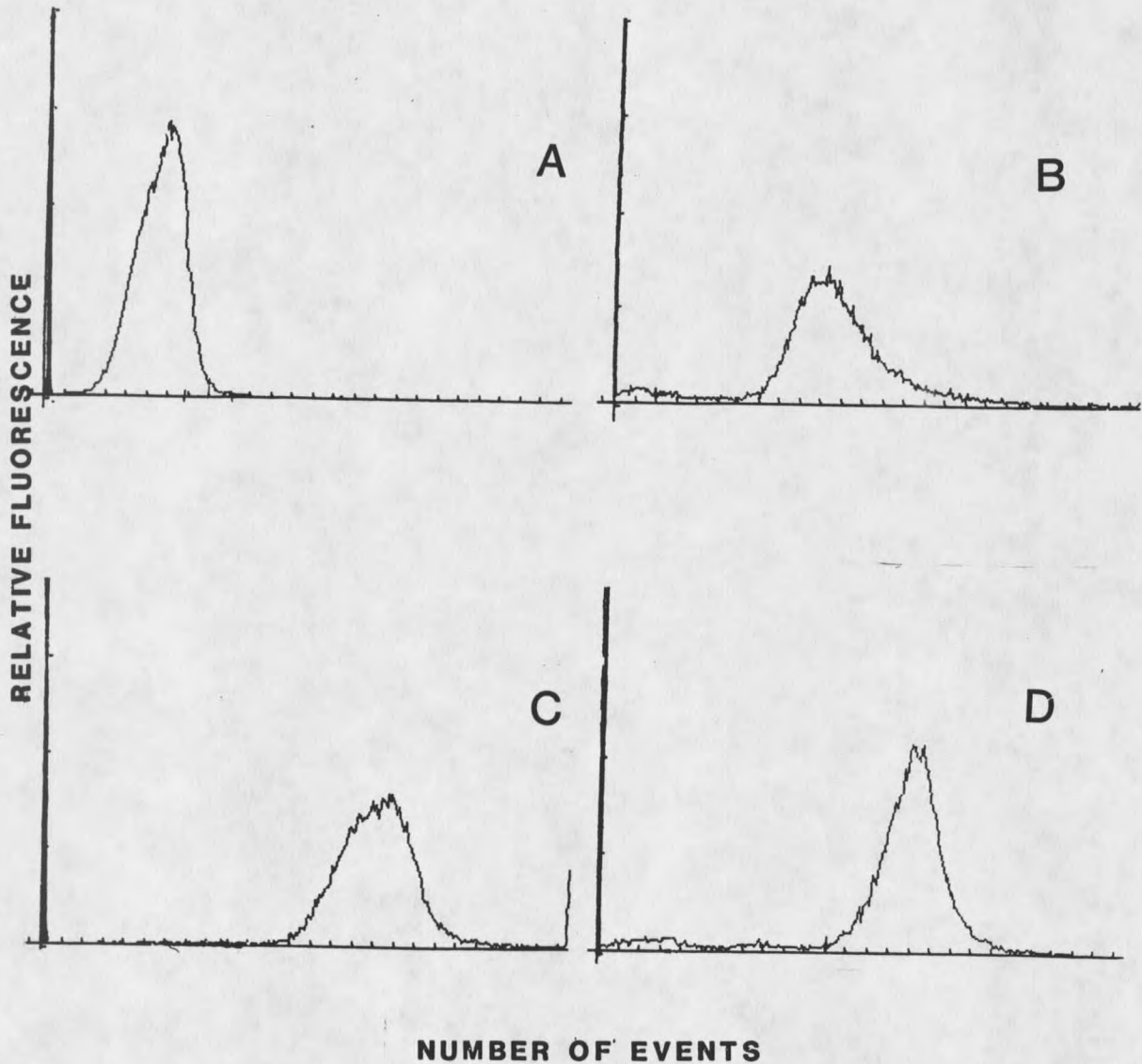


Figure 6. Histograms of Fluorescein Diacetate Activity. Number of events (linear scale) versus log of fluorescence intensity for (A) Chlorella autofluorescence, no FDA; (B) FDA-stained cells at time zero; (C) 7 hours; (D) 25 hours

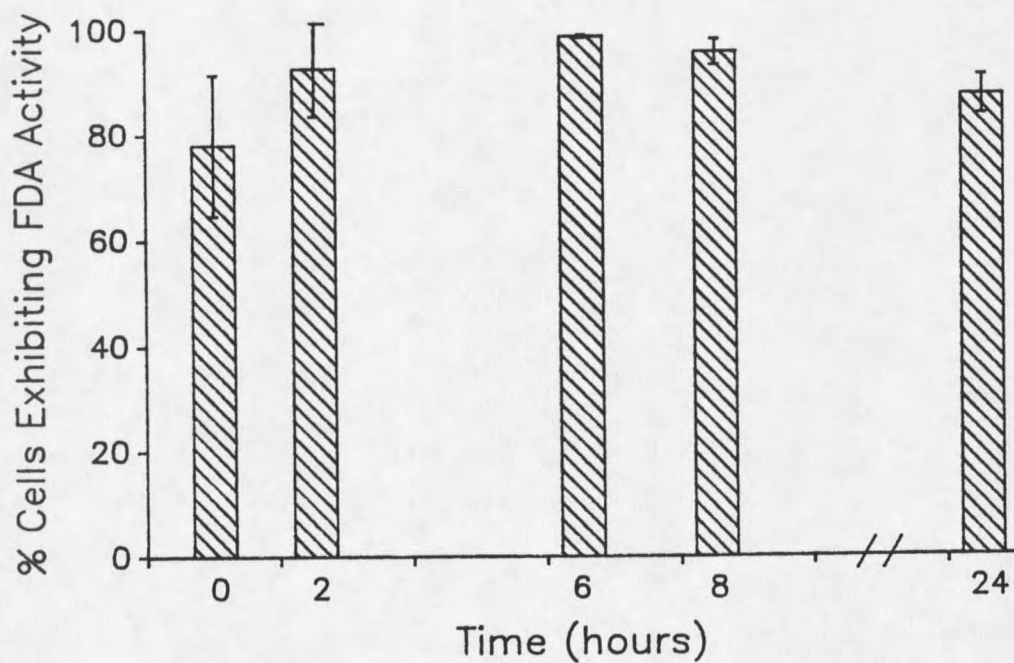


Figure 7. Bar Graph of Percent Viable Cells. Expressed as percentage of 10,000 flow cytometric events exhibiting esterase activity for cleavage and activation of Fluorescein Diacetate.

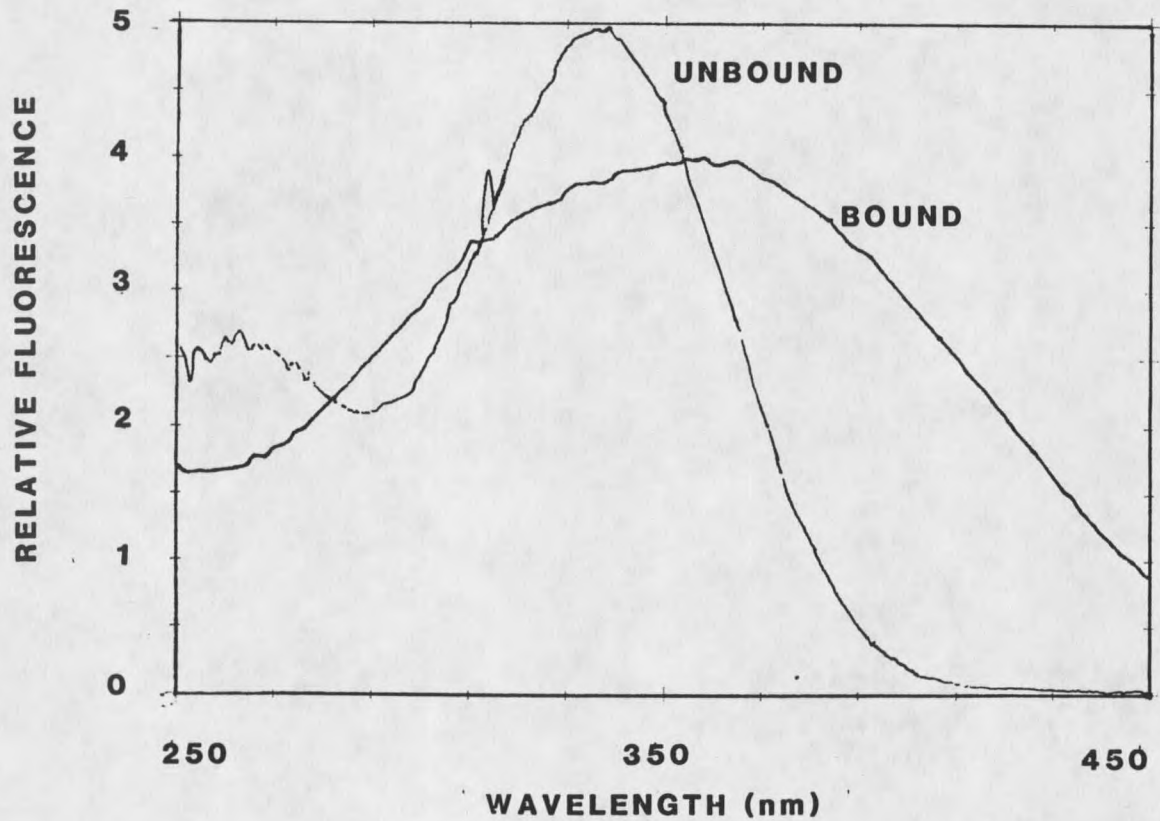


Figure 8. Relative Fluorescent Excitations of Unbound and Bound Hoechst 33258. Unbound stain was added to cell-free Bold's medium. Readings for bound Hoechst were obtained with whole Chlorella cells stained with 1 mM Hoechst. Excitation: Unbound 336 nm; Bound 357 nm.



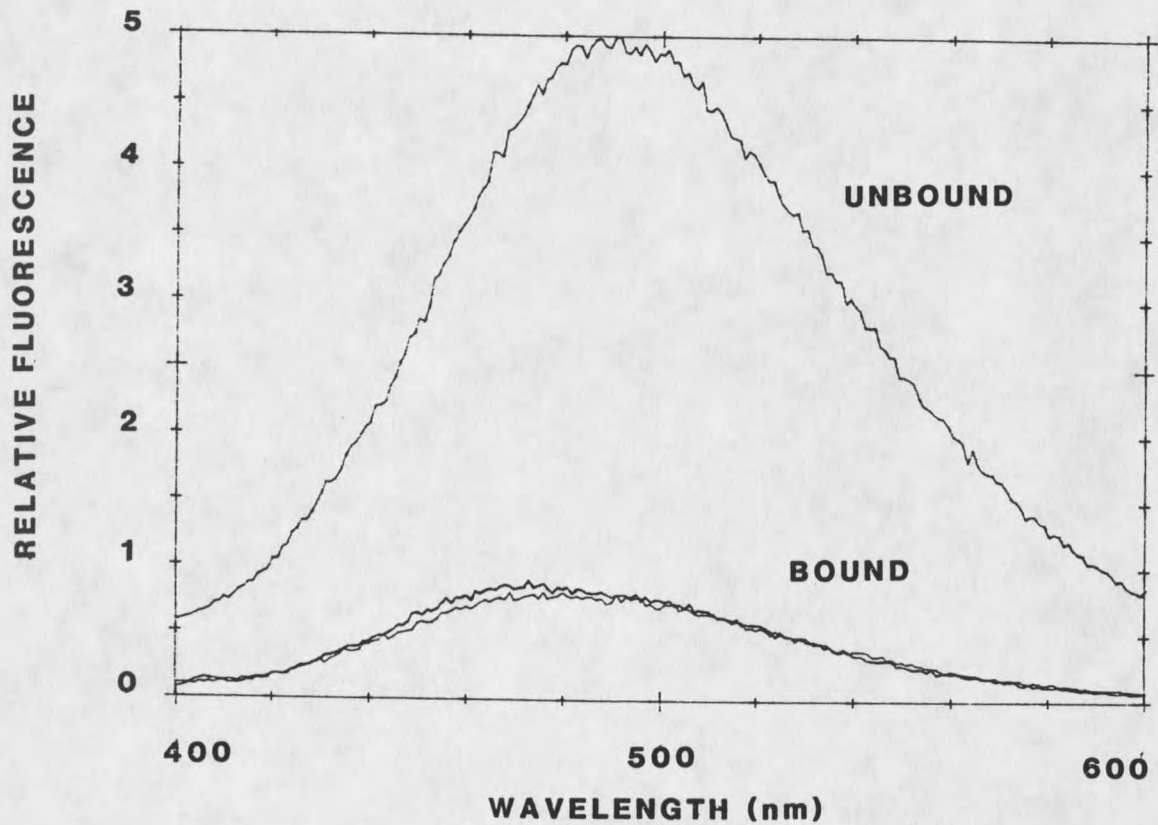


Figure 9. Relative Fluorescent Emissions of Unbound and Bound Hoechst 33258. Unbound stain was added to cell-free Bold's medium. Readings for bound Hoechst were obtained with whole *Chlorella* cells stained with 1 mM Hoechst. Emission wavelenths: unbound 490 nm; bound 471 nm.

stabilize (Figure 10). The fluorescence intensity of the Hoechst-DNA complex is stable indefinitely. Fluorescence intensities remained stable for cells analyzed three days after staining. Observations of fluorescence were not made beyond that point. A series of excitation and emission scans of Chlorella samples which received different numbers of washes by centrifugation revealed that the background fluorescence of the unbound dye is removed after three washes.

Cell Cycle Patterns of Triglyceride and  
DNA Levels Under Optimal Growth Conditions

In synchronized cultures grown at neutral pH and nutrient sufficiency ( $140 \text{ uE/m}^2 \text{ s}^{-1}$ ), a synthesis of TG occurred throughout the photosynthetic growth phase with utilization prior to cell division (Figures 11A & 11C). Relative levels of TG are expressed as Nile Red units per million cells. An increase in NR units, a synthesis stage, extended to the 8th hour. After this point, a decrease in Nile Red units, a utilization stage, was apparent (Figure 11A) just prior to the onset of cytokinesis (Figure 11C). Under these optimal, non-stressed conditions there was essentially no net accumulation of TG per cell at the end of one cycle. Observation of the level of Nile Red units per mL,

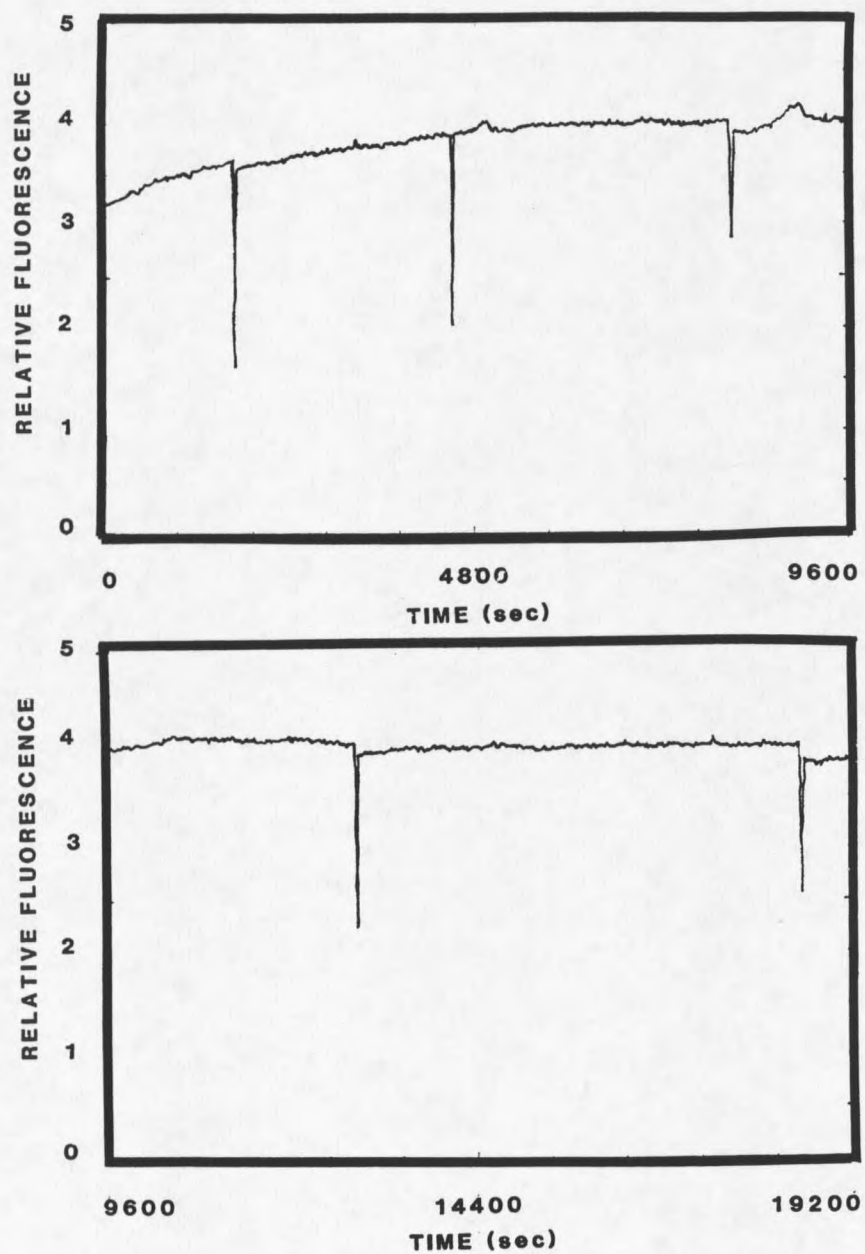


Figure 10. Time Course of Staining Chlorella with Hoechst 33258. Exc. 357 nm. Em. 471 nm.

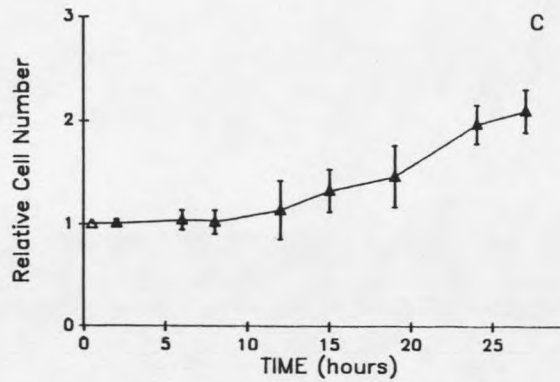
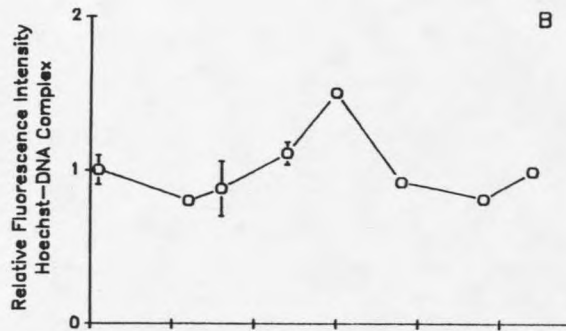
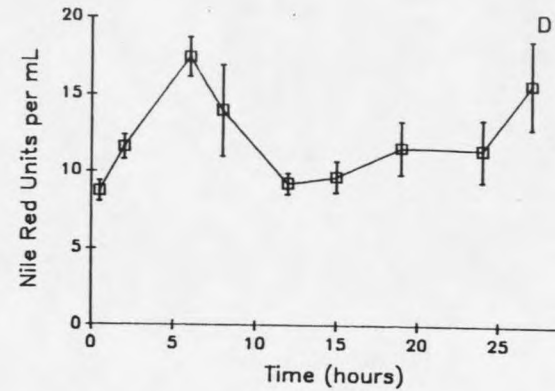
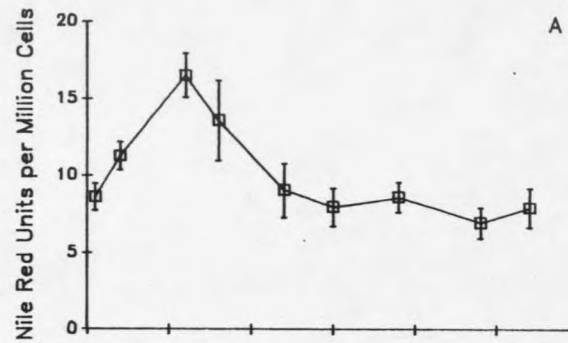


Figure 11. Cell Cycle of *Chlorella* CHLOR1 at neutral pH and no growth inhibitors. Patterns of triglyceride synthesis- utilization as measured by Nile Red response. (A) DNA expressed as fluorescence intensity of the Hoechst-DNA complex. (B) relative cell number. (C) Nile Red units per mL (D).

however, reveals that a synthesis of TG continues as the cells divide (Figures 11D & 11C).

DNA levels were quantified fluorometrically with the bisbenzimidazole dye, Hoechst 33258. A comparison of NR units with plots of relative cell number and DNA units per million cells serves in positioning the trends in TG levels within the cell cycle (Figure 11B). However, the peak in fluorescence of the Hoechst-DNA complex occurred at 15 hours, after the cells began to divide (Figures 11B & 11C). This phenomenon is believed to be an artifact of the cell enumeration procedure.

#### Visualization of Nile Red-stained

#### Triglyceride Droplets

In addition to providing a convenient method for quantifying TG patterns (Cooksey et al., 1987), the Nile Red stain also allows for a visual representation of the cellular location of TG storage droplets. When Nile Red interacts with the triglyceride droplets in microalgae it fluoresces yellow over the red background of chlorophyll autofluorescence (Figures 12 & 13). The increase in cell size and volume of lipid droplets provides visual verification of the synthesis-utilization patterns observed fluorometrically. Early in the cell cycle, the Chlorella cells are small exhibiting low Nile Red fluorescence (Figure 12). After 7.5 hours of growth, the

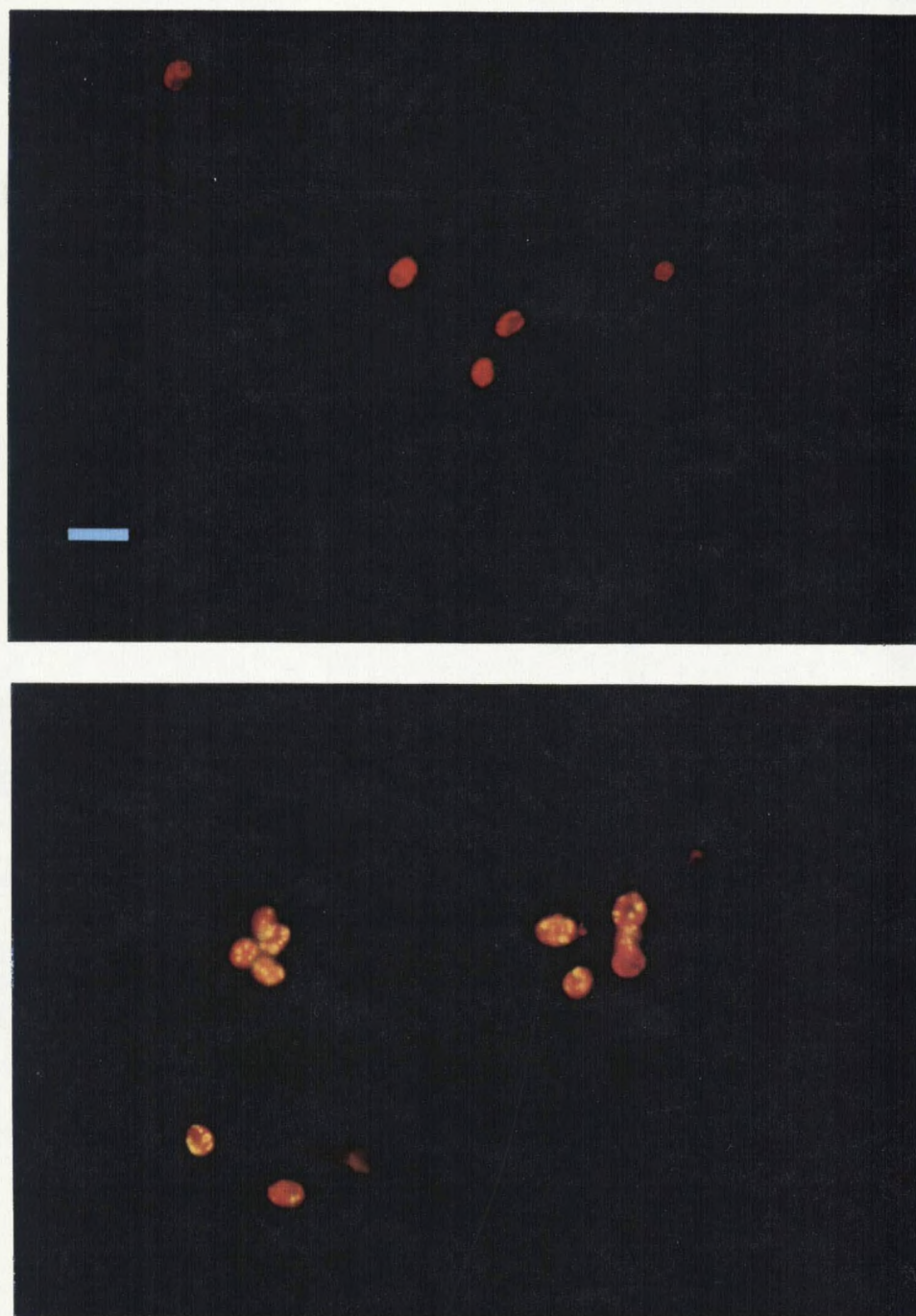


Figure 12. Fluorescent Micrographs of Nile Red-stained Chlorella at 0.5 hours (top) and 7.5 hours (bottom) in the cell cycle. Cells were cultured under optimum conditions of nutrient sufficiency and neutral pH. TG droplets fluoresce yellow against the red background of chlorophyll autofluorescence. 400x magnification. Scale bar = 10  $\mu$ m.

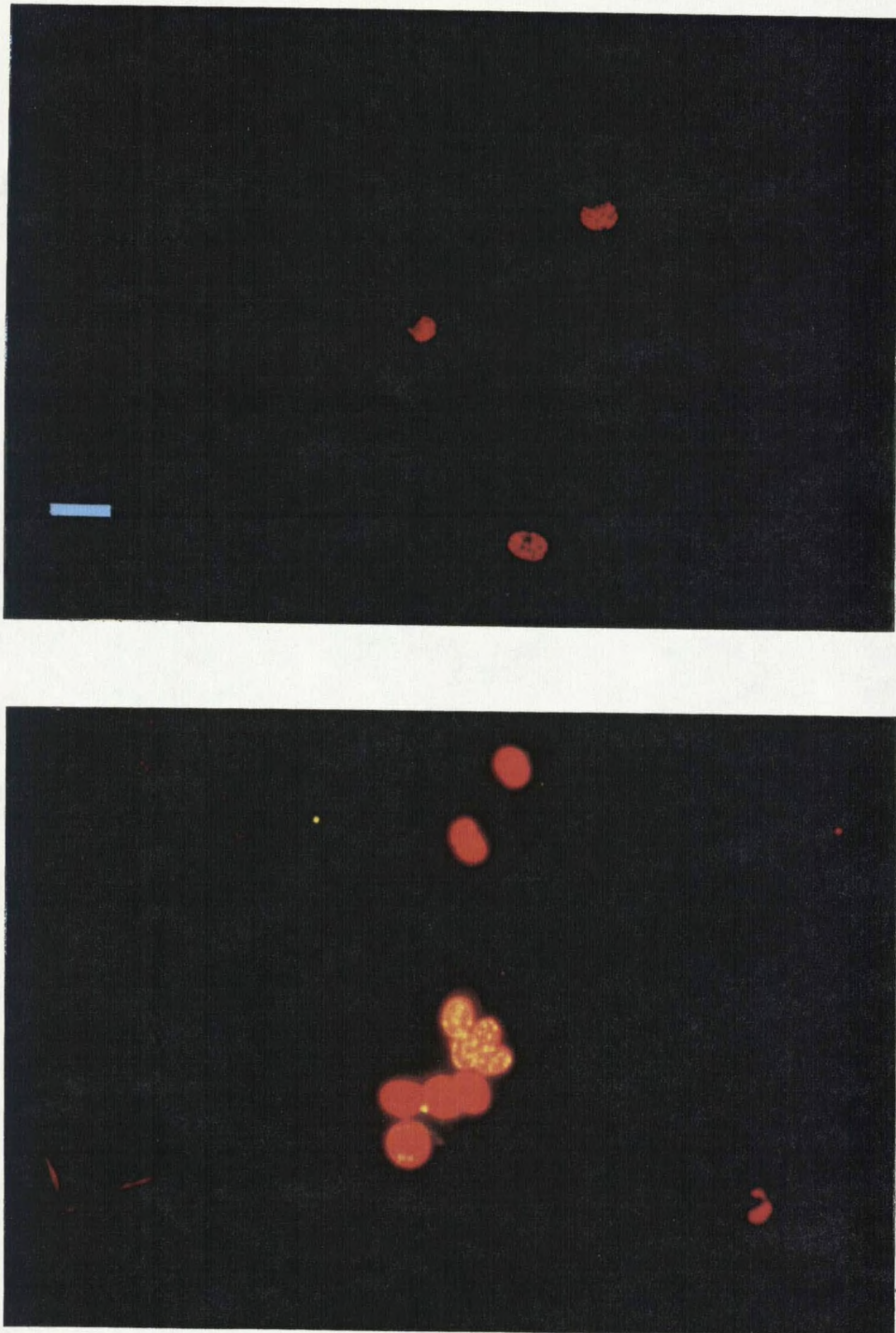


Figure 13. Nile Red fluorescence at 12 hours (top) and 31 hours (bottom) in the cell cycle of Chlorella cultured at optimal conditions.

cells are larger with a significantly higher level of TG (Figure 12). At 12 hours, the cells are increased in size yet diminished in NR fluorescence (Figure 13). By 31 hours, the cells have divided and have completed the cycle back to small cells with reduced TG levels (Figure 13). Although the cultures were subjected to the synchronization procedure, TG levels equivalent to the bulk population are not visually apparent in some of the cells (Figure 13).

#### Alkaline Stress Effects on Neutral Lipid Accumulation

Relative TG levels for the CAPS-buffered pH 10 cultures steadily rose to  $2.46 \pm 0.2$  relative NR units by the end of the 25 hour monitoring period while the cultures at neutral pH exhibited the synthesis-utilization pattern achieving a peak of  $1.64 \pm 0.1$  relative NR units at eight hours decreasing to  $1.24 \pm 0.3$  by 25 hours (Figures 14A & 14B). The pH 7 cultures experienced a doubling in cell number by 22 hours while the pH 10 cultures were arrested at the initial cell density of  $8.6 \times 10^5 \pm 8.6 \times 10^4$  (Figure 14C). These samples were precultured in the same incubator in which the experiment took place. As a result, they received a constant light flux of about  $120 \text{ uE m}^{-2} \text{ s}^{-1}$ .

Bacterial check plates revealed that the control series of cultures were contaminated with a Gram negative



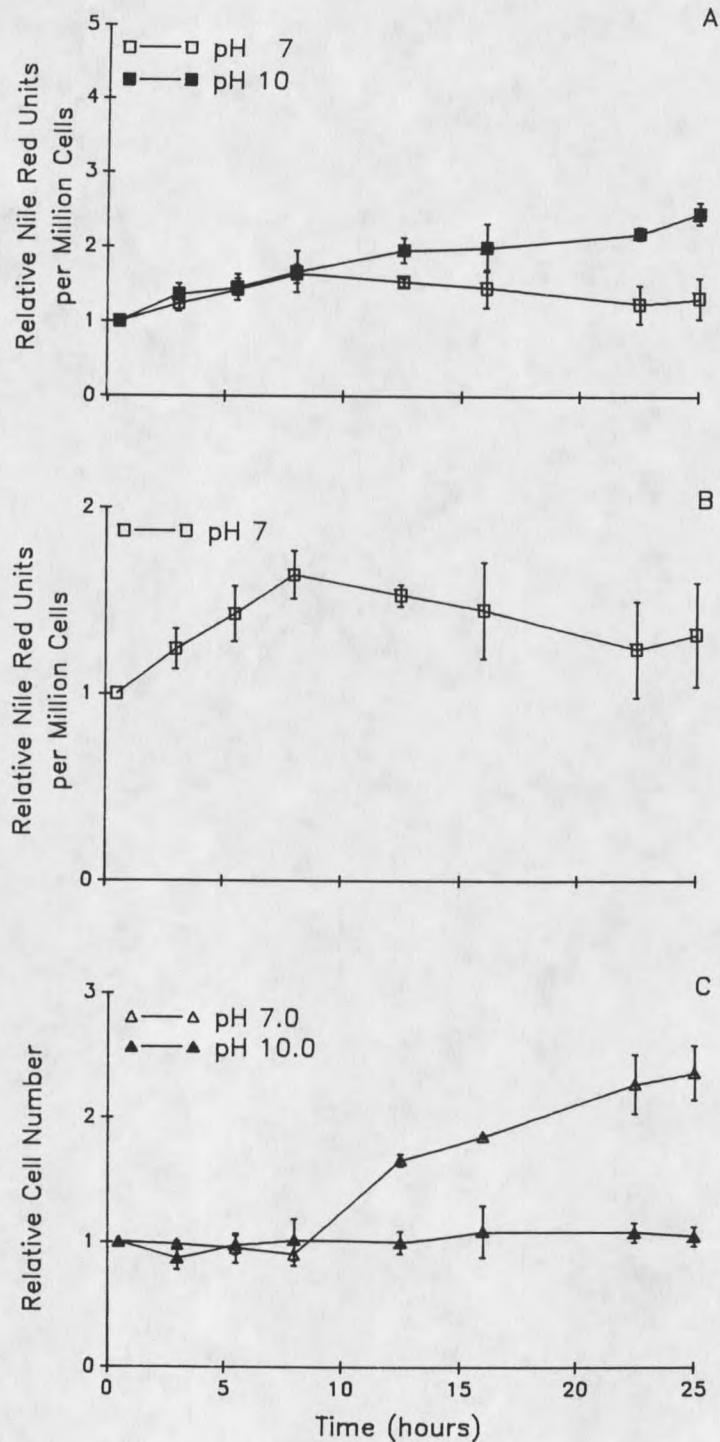


Figure 14. Alkaline Stress Effects on Cell Cycle and TG Levels. (A) NR units per million cells. (B) Nile Red units per million cells for control only -- expanded scale. (C) Relative cell number for control and alkaline-stressed cultures.

bacillus. Since all control flasks were contaminated, the bacillus was probably introduced at the beginning of the experiment by the parent culture from which the experimental samples originated. Since the decrease in NR units for the control samples (Figure 14B) was not as rapid as that seen in other experiments it was speculated that a nutrient stress condition may have been induced by bacterial activity. A spectrophotometric analysis for nitrogen remaining in the media at the end of the experiment revealed similar concentrations of nitrate ( $53 \pm 2$  mg/L for the control samples and  $48 \pm 6$  mg/L for the CAPS-buffered system) as compared to a nitrate concentration of 250 mg/L for fresh media (Figure 15).

An additional alkaline stress experiment was conducted in which cells were precultured at  $67 \text{ uE/m}^2 \text{ s}^{-1}$  until time zero when they were placed in an incubator operating with a light flux of  $145 \text{ uE/m}^2 \text{ s}^{-1}$ . In this experiment, the CAPS-buffered cultures synthesized TG to a maximum of  $5.52 \pm .79$  relative NR units by the 25th hour of incubation in continuous light while the cultures at neutral pH achieved a peak of  $1.49 \pm .08$  NR units at 8 hours decreasing to  $.57 \pm .08$  by 25 hours (Figure 16A). The synthesis-utilization pattern is more evident on the expanded scale (Figure 16B).

A burst in cell number occurred in this experiment in which preculturing was performed at low light intensities.

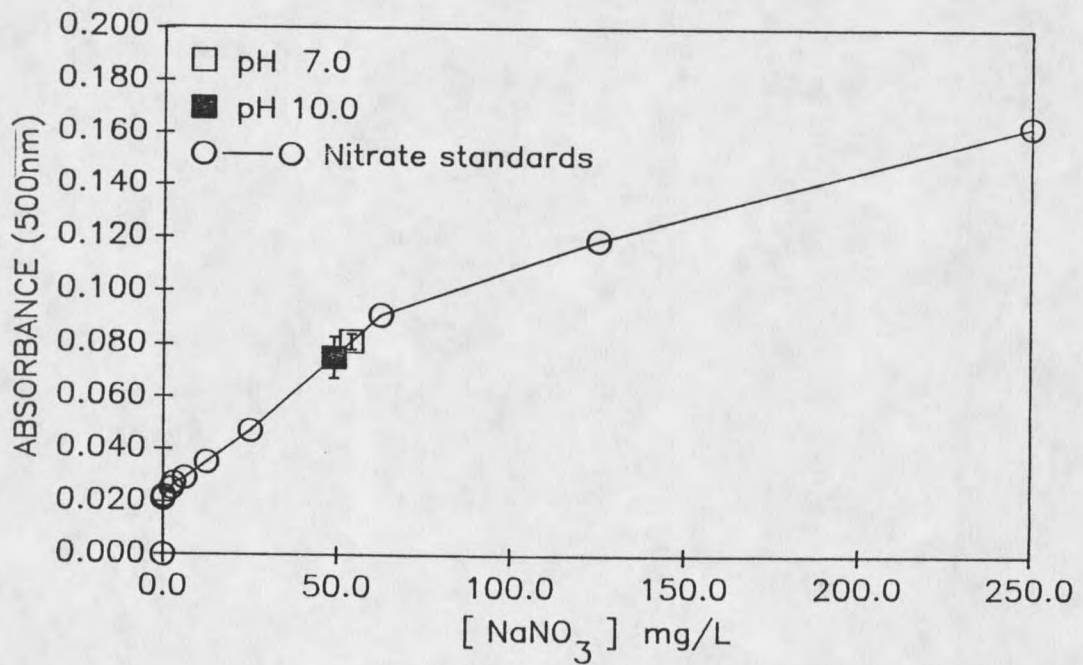


Figure 15. Calibration Curve for Spectrophotometric Determination of Nitrate Concentrations. Nitrate concentrations for bacterial contaminated pH 7 and pH 10 cultures are shown.

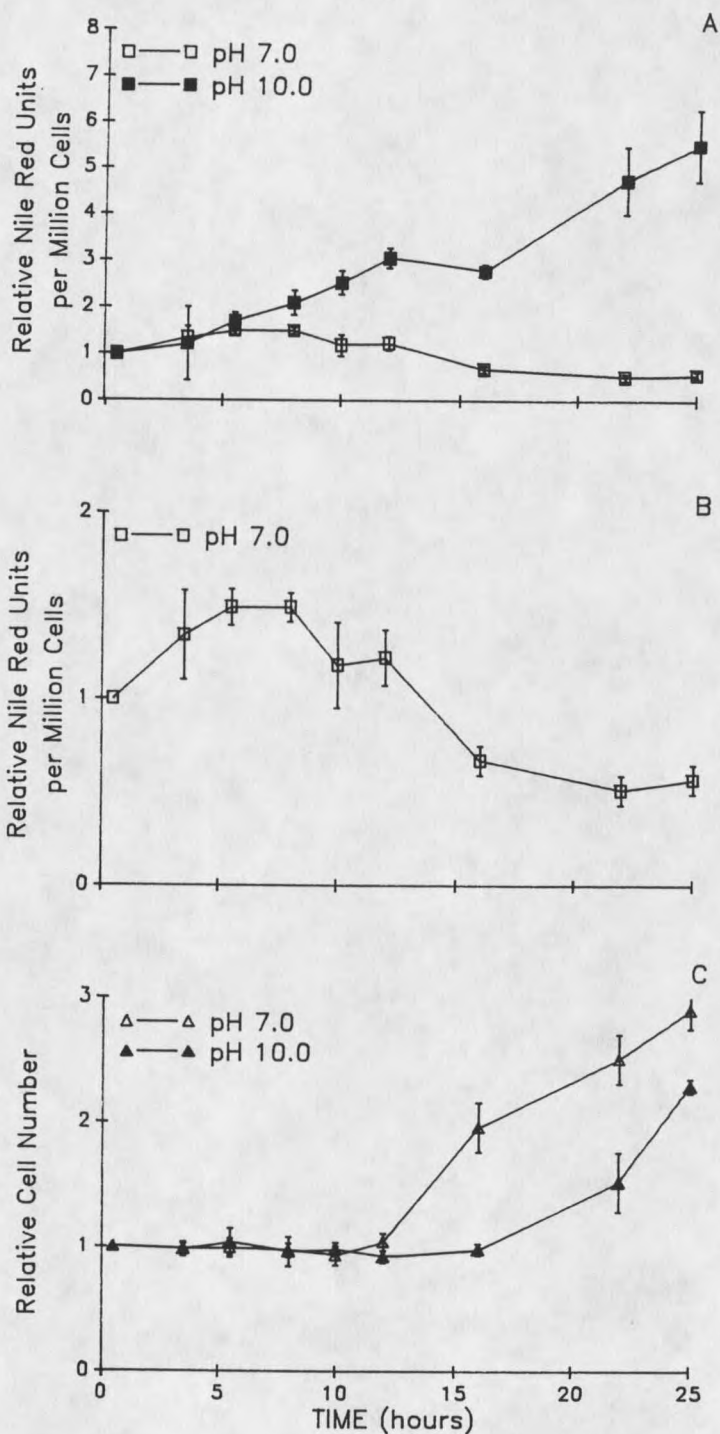


Figure 16. Cell Cycle Parameters for Alkaline Stress and Control Conditions at Elevated Light Levels. (A) Relative NR units per million cells. (B) Relative NR units for the pH 7 treatment on an expanded scale. (C) Relative cell number.

The pH 7 cultures reached a relative cell number of  $2.9 \pm 0.5$  by the 25th hour in an extended growth pattern which appeared to be approaching the quadrupling which has been reported for the cell cycle of Chlorella (Tamiya, 1963). The pH 10 cultures also experienced a burst in cell division although the growth of these cultures lagged behind the control cultures by about 5 hours (Figure 16C). Unlike the other experiments the samples in this experiment were precultured in the incubator with low light levels and experienced a burst of growth upon entering the light period in the higher light incubator.

#### Relative DNA Quantification by Flow Cytometry

Flow cytometric analyses of the relative fluorescent intensities of the Hoechst-DNA complex and forward scatter were performed for the HEPES and CAPS-buffered samples at each sample point throughout the monitoring period. Selected contour plots are presented for each treatment in Figures 17 and 18. The FACS histograms are scatterplots of Hoechst-DNA fluorescent intensity (on the vertical axis) versus forward scatter, a measure of cell size (on the horizontal axis). Both parameters are expressed on linear scales. Contour maps were drawn by connecting points with five or more events. The contour lines increment concentrically from 5 to 50 events per point,

pH 7

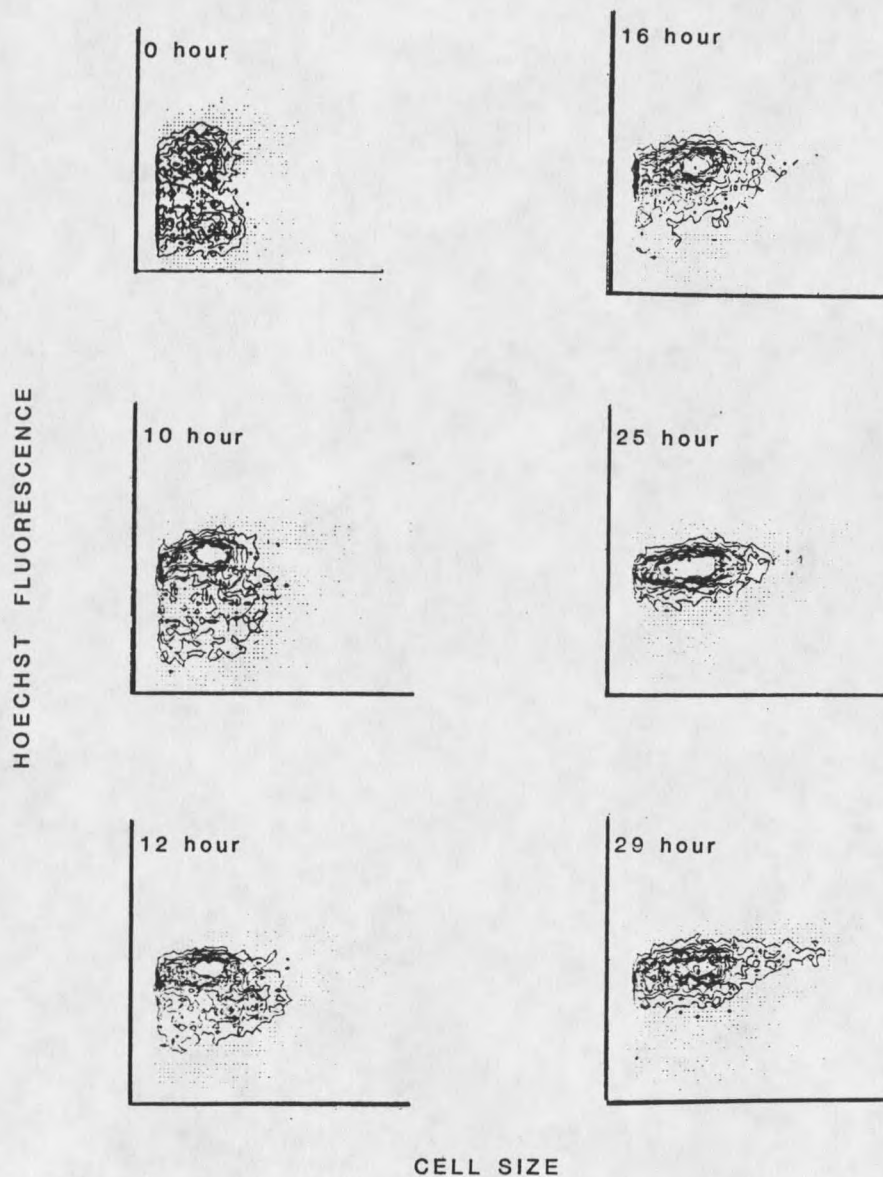


Figure 17. Fluorescence behavior of Hoechst-DNA in pH 7 cultures. Flow cytometer contour plot of Hoechst fluorescence versus forward scatter, a measure of cell size. Both parameters are plotted on linear scales.

pH 10

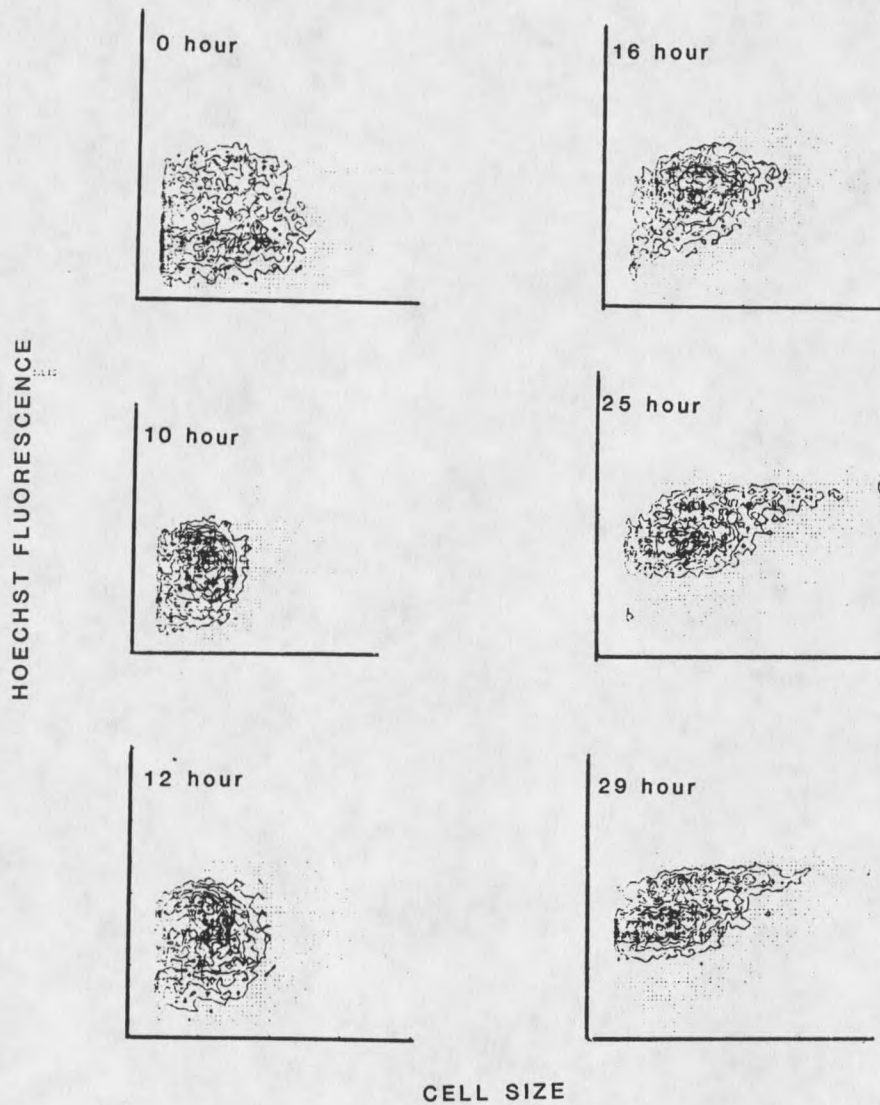


Figure 18. Fluorescence behavior of Hoechst-DNA in pH 10 cultures. Flow cytometer contour plot of Hoechst fluorescence versus forward scatter, a measure of cell size. Both parameters are plotted on linear scales.

with the bulk of the population lying in the center of the map.

Starting at time zero for the pH 7 treatments (Figure 17), a fairly narrow distribution of cell sizes is evident as are two distinct populations of DNA intensities, one roughly double the intensity of the other. As the cycle progresses through hours 10 and 12, a consolidation of the cells at the higher intensity is evident, although cell size increases only slightly. By the 25th hour, the cells are essentially all at the doubled DNA intensity level, with a broader distribution of cell sizes. It is at this point that the growth curve (Figure 16C) indicates cytokinesis has occurred and we would expect a decrease in both cell size and DNA intensity. At the 29th hour the cells still appear to be in the higher DNA state although the size distribution has expanded considerably. The scatterplots for the pH 10 samples (Figure 18) are similar to those at pH 7 (Figure 17) although the cells at pH 10 lagged somewhat in cell cycle progression. This phenomenon was also apparent in the growth curves for the two culture treatments (Figure 16C).

Translation of the number of fluorescent events appearing in each fluorescence level to a percentage basis helps to illustrate the presence of two distinct populations of fluorescent events (Figure 19).



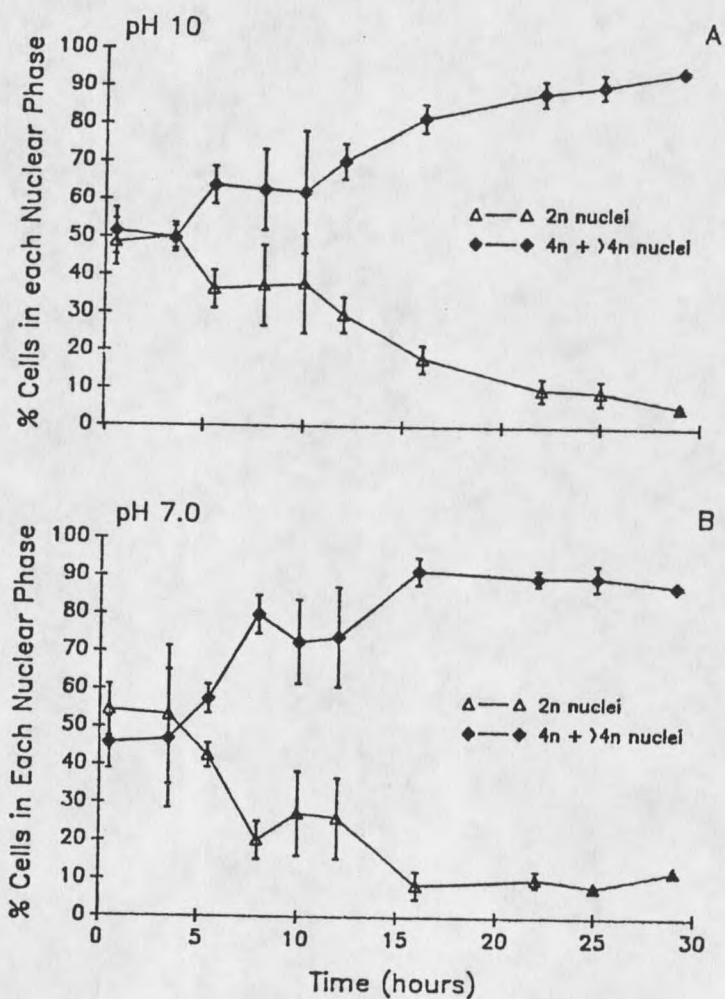


Figure 19. Percentages of Cells at the '2n' and '4n' Hoechst Fluorescence Levels for Control and Alkaline-stress Conditions. '2n' and '4n' are arbitrary designations for two populations of fluorescent events observed by flow cytometry.

The percentages of events residing at each fluorescence level are presented in Figures 19A and 19B. The status of the nuclei in the populations at the lower and higher fluorescent intensities have been arbitrarily designated "2n Nucleii," and "4n Nucleii" respectively. At time zero, the cultures are composed of approximately equal percentages of cells in each nuclear stage. As the cell cycle progresses, a departure of cells from the "2n" stage to consolidation at the "4n" stage is occurs for both culture treatments (Figures 19A and 19B).

#### Nitrate and Calcium Deficiency

Nile Red units and cell concentration were monitored at 10 points during a 36 hour period for nitrogen-deficient, low calcium, and control cultures (complete media). After 36 hours of growth, the nitrate-deprived cells achieved a relative increase in Nile Red units per million cells of  $1.4 \pm 0.1$  times the initial NR level (Figure 20). The nutrient-sufficient control cultures displayed a typical synthesis-utilization pattern reaching a maximum relative Nile Red units per million cells of  $1.4 \pm 0.1$  at the eighth hour sample point (Figure 20B). The relative Nile Red units per million cells of the calcium-deficient cultures were relatively constant throughout the 36 hour monitoring period (Figure 20A). All cultures grew during this interval although the control cultures doubled

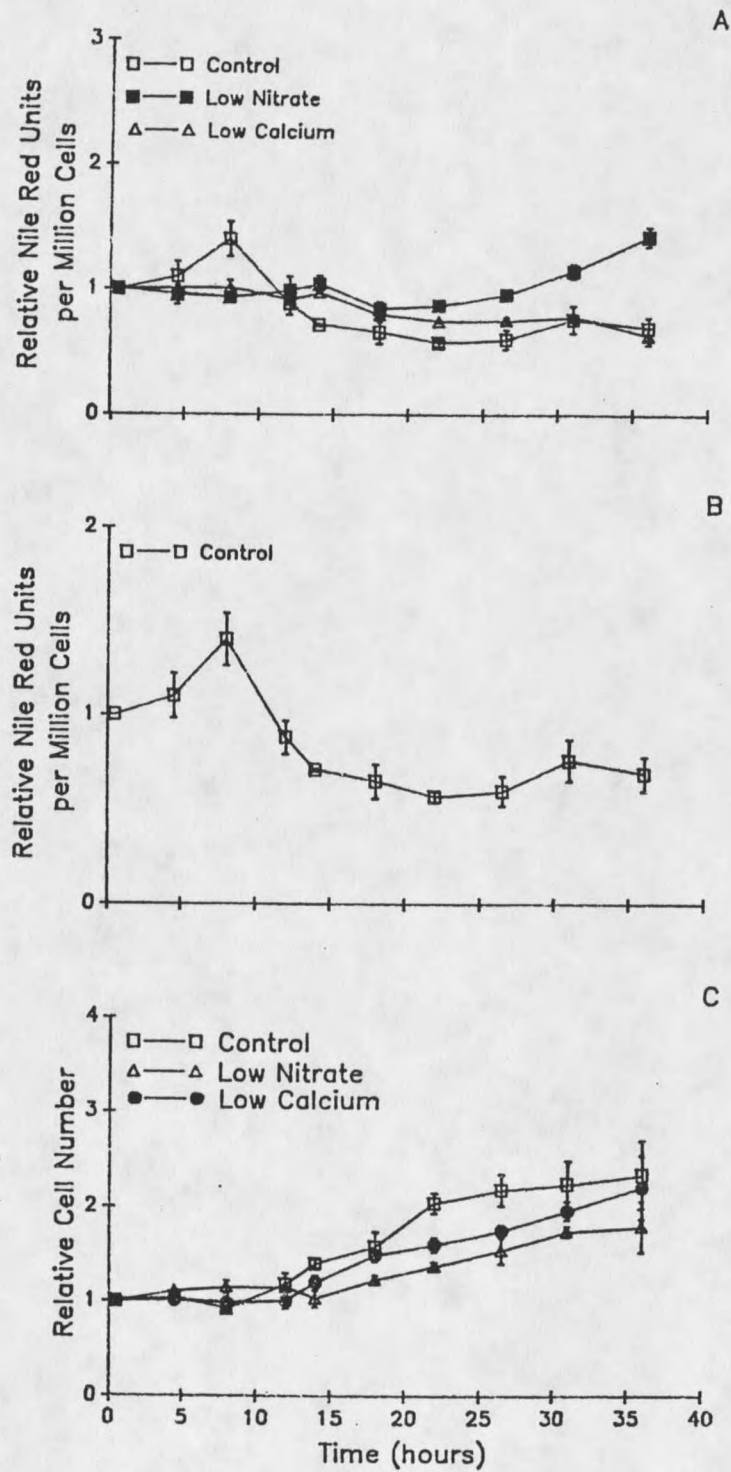


Figure 20. Relative Nile Red (A & B) and Relative Cell Numbers (C) for Low Nitrogen, Low Calcium, and Control Cultures.

in cell number most quickly (reaching a relative cell number of  $2.0 \pm 0.1$  by 22 hours) (Figure 20C). The low calcium cultures lagged in growth somewhat behind the control cultures not achieving a doubling in cell number until 36 hours ( $2.2 \pm 0.3$ ) (Figure 20C). The nitrogen-deficient cultures lagged significantly completing the 36 hour monitoring period with only a  $1.8 \pm 0.3$  relative increase in cell number (Figure 20C).

The nitrate and calcium concentrations found in the three different treatment conditions at zero and 36 hours are presented in Table 3.

Table 3. Nitrate and Calcium Concentrations

Treatment	Incubation Time (h)	Total Calcium mg L <sup>-1</sup>	Nitrate mg L <sup>-1</sup>
Control	0	5.1	$0.21 \pm .04$
Control	36	4.1	0.09
Calcium free	0	N.D.*	--
Calcium free	36	$0.37 \pm 0.3$	--
Nitrate free	0	--	0.02
Nitrate free	36	--	$0.02 \pm .001$

Note: pH values for all media were 6.9 at time zero. \*N.D. = None Detected. Approximately 50 mL of each sample were analyzed for total calcium. Values represent concentrations for one sample except for those where a standard deviation is included. In these instances two samples were analyzed.

Cell growth and Nile Red responses were observed through the fourteenth day of incubation with continuous light. The Nile Red signal of the nitrogen-deficient cultures continued to rise to a maximum of 2.53 relative NR units per million cells (Figure 21A) despite a very minimal increase in cell number (Figure 21C). The low calcium and control cultures exhibited no net accumulation of TG throughout the 14 day period (Figures 21A & 21B) although an increase in relative cell number of roughly 20 times the concentration of the day zero cultures was achieved before the cultures entered stationary phase of growth (Figure 21C). Micrographs of Nile Red stained cultures illustrate the visual differences in cell morphologies and neutral lipid contents in the 14 day control, calcium deficient, and nitrogen deficient cultures (Figures 22 & 23). Cells in the control and low calcium media were essentially identical in morphology.

#### TCA Inhibition with Monofluoroacetate

The HEPES-buffered MFA-inhibited cells experienced a continuous and dramatic increase in TG levels throughout the 24 hour monitoring period (Figure 24A). In contrast, the control samples, revealed the same synthesis-utilization pattern seen in earlier studies of cells growing under optimal conditions (Figure 24B). The MFA-treated cells achieved a  $3.2 \pm .04$  fold relative increase

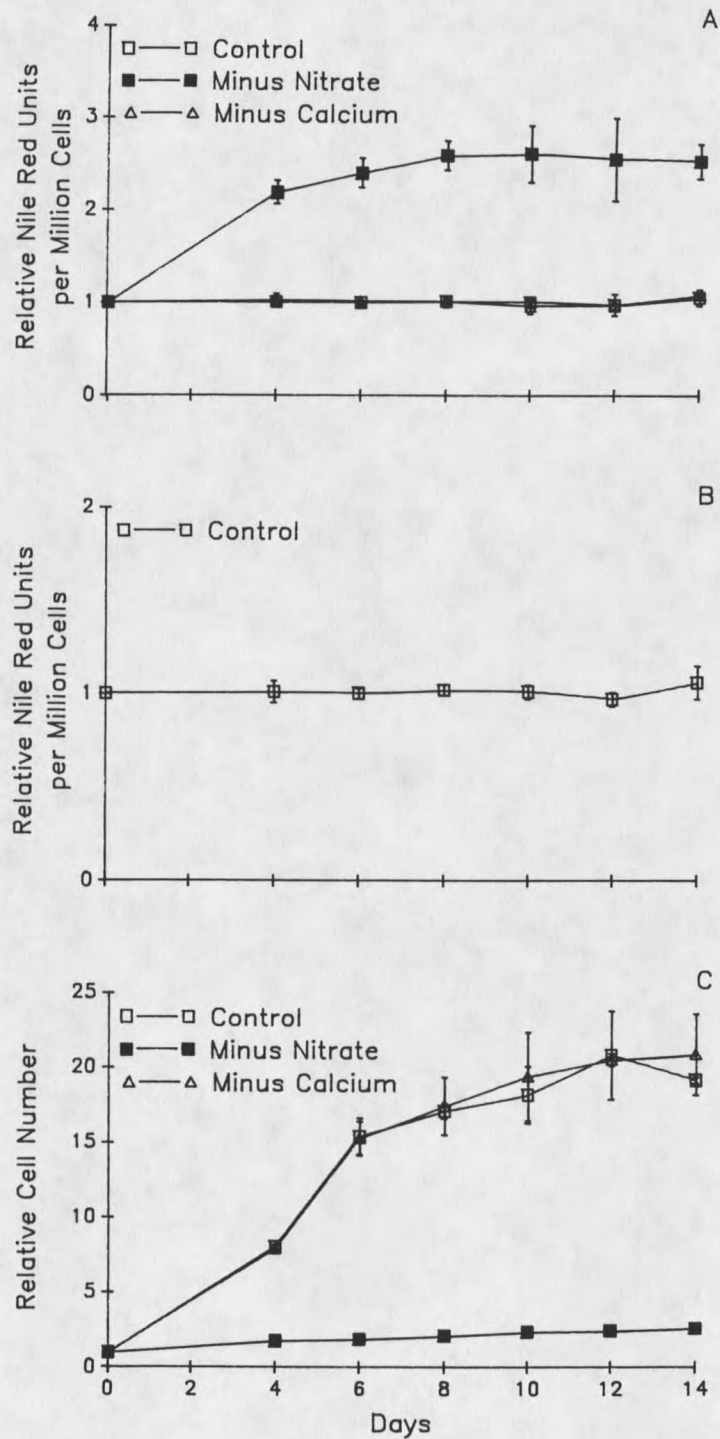


Figure 21. Relative NR units (A & B) and Relative Cell Numbers (C) for Low Calcium, Low Nitrogen and Control Cultures from 0 to 14 days.

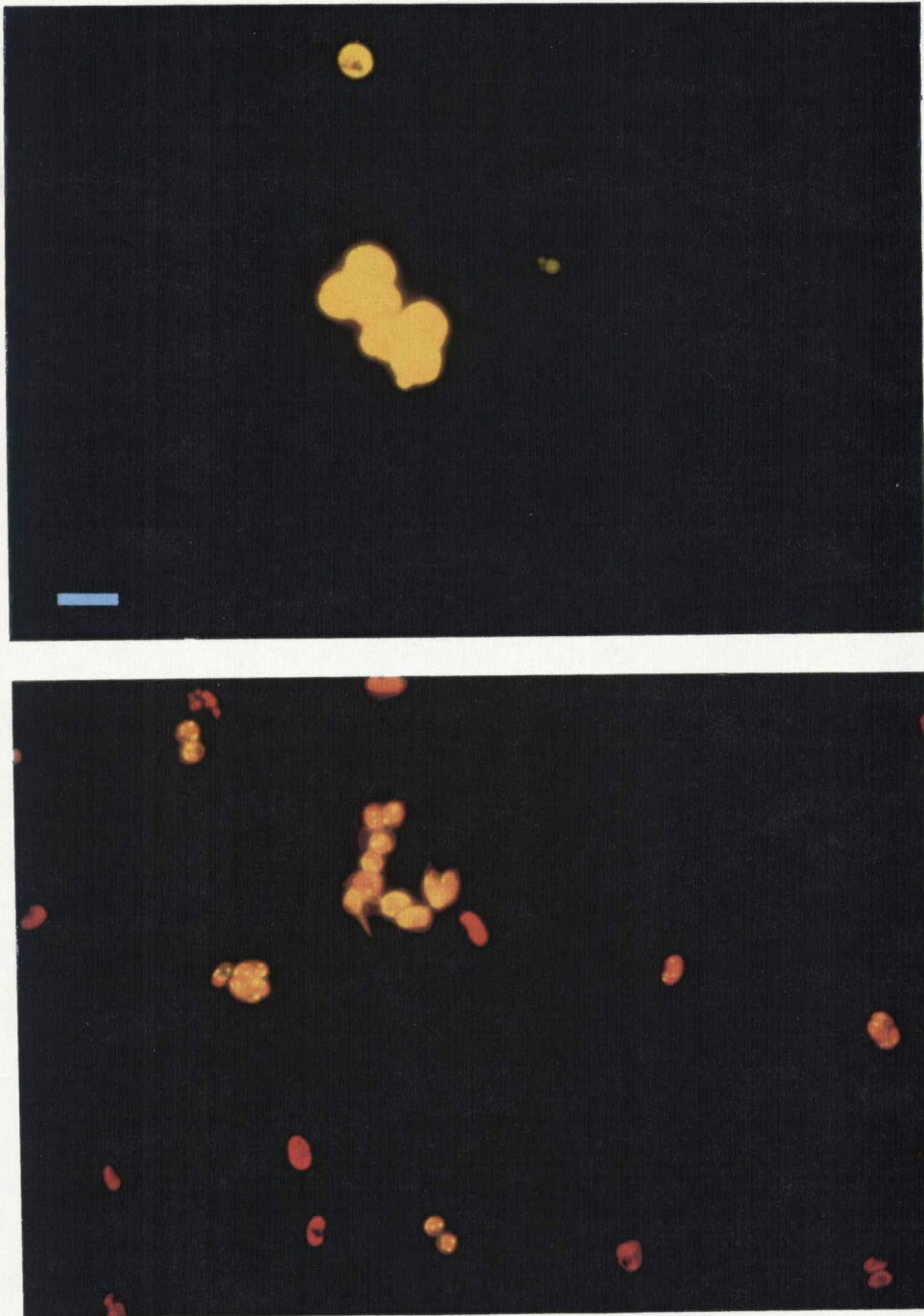


Figure 22. Fluorescent Micrographs of Nile Red Stained Low Nitrogen and Low Calcium Cultures at 14 Days. Nitrogen-deprived cells (Top) Cells at low calcium (Bottom). 400x magnification. Scale bar = 10  $\mu$ m.































































































